



Pitfalls in OCT Imaging

Eunoo Bak

Abstract

Optical coherence tomography (OCT)-based imaging of the optic nerve head, retinal nerve fiber layer, and the ganglion cell complex has become a key tool in the diagnosis and evaluation of glaucoma. The structural details available from OCT continue to improve with advances in technology. However, artifacts and misinterpretation of OCT still can lead to clinical misdiagnosis of glaucoma. Owing to the “floor effect” of retinal imaging, red and green disease may lead to erroneous results. Common OCT artifacts are classified as (1) patient-related factors (e.g., myopia, media opacities, vitreoretinal interface problems, optic nerve head pathologies, motion artifact, blink artifact); (2) instrument factors (e.g., poor image quality or device performance, inaccurate optic disc margin delineation, segmentation errors); and (3) operator factors (e.g., incorrect scan-circle placement, incorrect axial alignment). Understanding the potential limitations and pitfalls of each instrument is imperative in patient care.

Keywords

Glaucoma · Optical coherence tomography
Artifact · Segmentation error · Red disease
Green disease

1 Introduction

Optical coherence tomography (OCT) is a noninvasive imaging modality that has become a useful ancillary tool for diagnosis and monitoring of glaucoma. It is widely used by ophthalmologists worldwide in daily practice, and they are now basing their treatment plans on OCT results for early glaucoma patients and glaucoma suspects (Stein et al. 2012; Gabriele et al. 2011; Dong et al. 2016). Despite the improvements in OCT technology, the user must be able to accurately interpret the data and be aware of potential artifacts and limitations that can lead to a false-positive or false-negative diagnosis.

Previous studies with various Spectral-domain OCT (SD-OCT) instruments have reported that over a quarter of patients may have artifacts of the retinal nerve fiber layer (RNFL) and/or ganglion cell-inner plexiform layer (GCIPL) complex analysis (Giani et al. 2010; Sull et al. 2010). Errors either in data acquisition or software analysis may result in artifacts of RNFL measurements, which may lead to inaccurate clinical

E. Bak (✉)

Department of Ophthalmology, Seoul National University College of Medicine, Seoul, Korea

Department of Ophthalmology, Seoul National University Hospital, Seoul, Korea
e-mail: eunoobak@snu.ac.kr

assessment. It takes time for users to understand the potential limitations and pitfalls of OCT. Regardless, understanding these limitations and being able to distinguish artifacts from true disease are imperative in patient care and can prevent further unnecessary, expensive investigations.

This chapter is devoted to the common artifacts affecting OCT that can lead to diagnostic errors.

2 Causes and Classification of OCT Artifacts

2.1 Floor Effect

In retinal imaging, the “floor effect” is defined as the point at which no further structural damage can be detected. Given this effect, OCT measurements are less useful for measuring tissue thickness in cases of advanced disease (Mwanza et al. 2015), possibly due to the presence of residual tissue (e.g., glial cells, blood vessels, nonfunctioning ganglion cell axons) or failure of tissue segmentation algorithms (i.e., artifactual floor) (Asrani et al. 2014). Thus, even though an advanced disease may be progressing, it is often challenging to detect identifiable changes with OCT. Disease monitoring in these eyes should not depend solely on optical imaging but must rely on standard automated perimetry or other visual function tests.

2.2 Red and Green Disease

Red and green are the main colors used in the OCT platforms to indicate that the results are within normal limits (within the 5–95% prediction interval) or abnormal (less than 1% prediction interval) when compared with the normative database. “Red disease” is a false-positive diagnosis, where the software mistakenly identifies an eye as abnormal even though there is no glaucomatous damage (Asrani et al. 2014; Chong and Lee 2012). In contrast, “green disease” is a false-negative diagnosis, when the software interprets

actual glaucomatous damage as normal (Sayed et al. 2017). Green disease artifacts can present as the result of the averaging of sectors that include a subtle notch in the RNFL, or an RNFL defect in an eye that started with a high value of RNFL thickness. In addition, RNFL can become thicker in eyes with RNFL edema, which can mask RNFL thinning (Moore et al. 2015). Clinicians therefore should not rely solely on the color scheme to interpret an OCT report. Also, they are encouraged to keep in mind that the red and green colors in OCT evaluations depend on the normative database of the manufacturer, which commonly includes only 300–500 patients. Depending on the manufacturer, these normative databases mostly do not include children, high refractive error, diverse races, or corrections for such variations. This may lead to erroneous results for some patient groups.

2.3 Classification of OCT Artifacts in Optic Disc Scan Analysis

The rates, types, and causes of OCT artifacts can vary according to the methods used for their definition and classification. OCT artifacts are classified as follows: (1) patient-related factors, (2) instrument factors, and (3) operator factors (Asrani et al. 2014; Han and Jaffe 2010). If no definite patient-related artifact is identified and the artifacts did not show any association with the operator, the cause of the artifact can be classified as an instrument error. However, there is a large overlap among these categories (i.e., scan artifacts often result from a combination of patient-related, instrument, and operator factors).

3 Patient-Related Factors

These are the most common causes and most confusing artifacts. It is common to see red areas in the results of a reliable good-quality OCT scan in a routine eye exam performed on a healthy person with no ocular disease. Some of these patients are diagnosed with glaucoma and

start on medical therapy. The person diagnosed requires lifelong treatment and follow-up, which leads to a psychological burden both to the patient and the family. In order to avoid misinforming patients, ophthalmologists must be able to differentiate among the common artifacts and anatomical variants that can lead to errors on OCT reports.

3.1 Split Bundle

In the majority of individuals, the superior and inferior poles of the optic nerve head receive the largest number of retinal ganglion cell axons in the form of two thick bundles. This configuration is the basis for the color-coded normative database comparisons of temporal–superior–nasal–inferior–temporal (TSNIT) profiles. In some individuals, the superior and/or inferior RNFL bundles are divided in two and enter the optic disc in the form of a pair of separate bundles each, thus masquerading as a local RNFL defect. This is called a split RNFL, which is an anatomical variant rather than an imaging artifact (Kaliner et al. 2007; Colen and Lemij 2001) (Fig. 1). This finding is one of the most common reasons for red disease in younger patients with good-quality OCT scans. A careful evaluation of the RNFL TSNIT profiles, lack of optic nerve head parameter abnormalities, normal macular ganglion cell analysis, and typical split RNFL images on RNFL thickness maps are important clues for correct diagnosis.

3.2 Myopia

Myopic eyes with longer axial length are associated with a higher percentage of abnormal diagnostic classifications, because the RNFL normative databases are typically adjusted only by age and not by axial length or refractive error (Qiu et al. 2011; Yoo et al. 2012). The normal population database used by the manufacturer specifically excludes subjects with high refractive error, which usually encompasses spherical equivalents between -5.00 and $+5.00$.

The overall RNFL thickness in high-myopic refractive error, typically with longer axial length, is thinner compared with the normal population (Budenz et al. 2007; Kang et al. 2010; Leung et al. 2006; Savini et al. 2012; Wang et al. 2011). In addition, hyperopia and shorter axial eye lengths show increases in RNFL thickness (Savini et al. 2012). These findings are attributed to the ocular magnification effects of axial eye length. When adjusting for ocular magnification, the negative correlation between these OCT measurements and both axial eye length and refractive error is removed (Savini et al. 2012; Leung et al. 2007). Moreover, the effects of axial-length magnification remain in patients who have undergone refractive surgery and cataract operation. When their axial eye length is unknown and their preoperative status is unrecognized, incorrect interpretation of OCT may result. Because most current OCT machines do not account for ocular magnification, patients with long or short axial eye lengths will have artificially low or high OCT measurements, respectively, when compared with the normative database. If the axial eye length is known, the OCT measurements can be corrected with the modified Littmann formula, as described by Bennet et al. (1994). However, in pathological myopia, true retinal thinning, such as myopic retinal schisis affecting the peripapillary RNFL thickness, may be present.

In addition to the changes of overall RNFL thickness, the peaks on the TSNIT RNFL thickness plot are shifted temporally toward the fovea in myopes relative to the general population (Kang et al. 2010; Hong et al. 2010; Hwang et al. 2012; Yamashita et al. 2014) (Fig. 2). Due to the more temporal shift of the RNFL peaks in myopia, the temporal RNFL thickness may be elevated, and the superior and inferior RNFL thicknesses may be reported as decreased (Wang et al. 2011; Yamashita et al. 2013). In other words, the thickness of RNFL bundles is normal, but with an abnormal topographic position. Hong et al. stated that RNFL peaks may deviate in normal individuals, leading to red disease artifacts, which have been associated with myopia and increased axial length (Hong et al. 2010). Hood

ONH and RNFL OU Analysis: Optic Disc Cube 200x200

OD ● ● OS

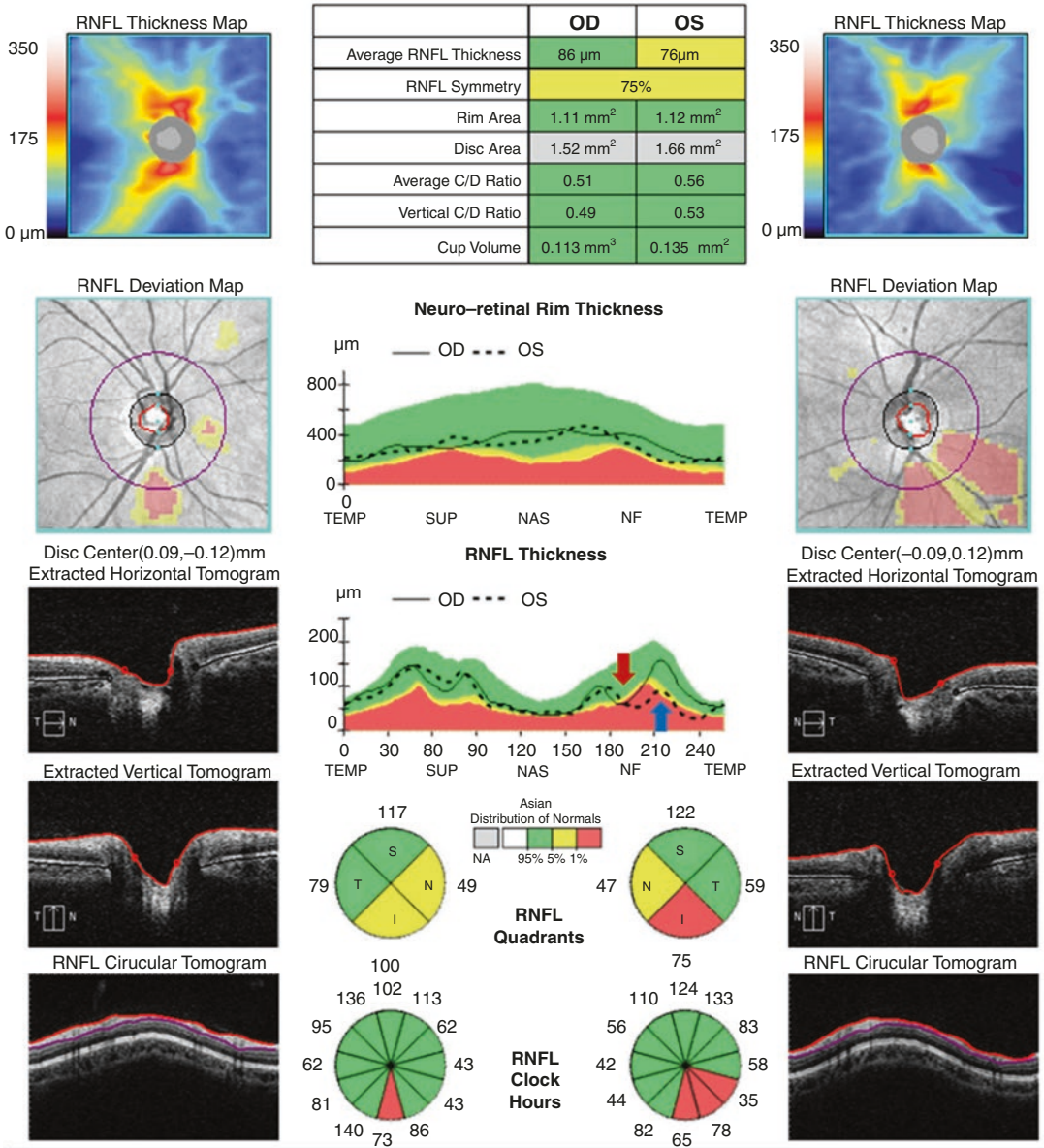


Fig. 1 Inferior RNFL bundle of right eye showing split RNFL defect. On the TSNIT profile, the inferior vertex is split into two peaks separated by a valley (red arrow). The

left eye shows a glaucomatous RNFL defect in the infero-temporal area (blue arrow)

et al. (2010) stated that the positions of RNFL peaks on TSNIT graphs are in the same regions as major retinal vessels. Careful examination of the RNFL TSNIT profile and major retinal ves-

sels, as combined with the optic nerve head parameters and macular scan results, is important for the recognition of these anomalies.

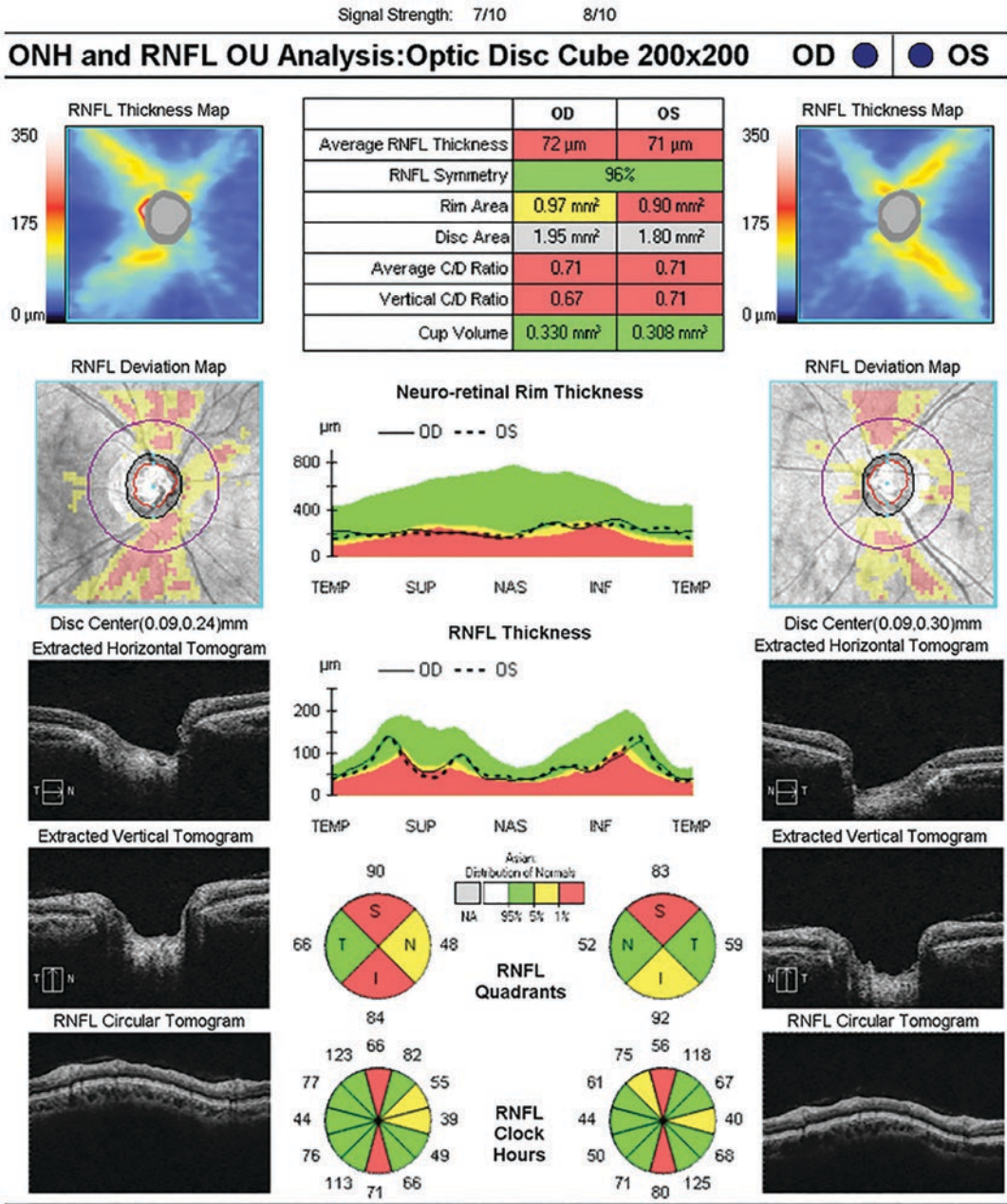


Fig. 2 Low values of RNFL thickness in nasal sectors on TSNIT profile of myopic patient due to temporal displacement of RNFL peaks. This occurred because the peaks did

not align with the expected positions in the TSNIT graphs based on the normative database

3.3 Peripapillary Atrophy

Peripapillary atrophy, which frequently accompanies myopia, is another cause of OCT segmen-

tation error (Fig. 3). This is clinically important, because peripapillary atrophy is found commonly in glaucoma patients (Jonas et al. 1989). Peripapillary atrophy occurs mostly with time-

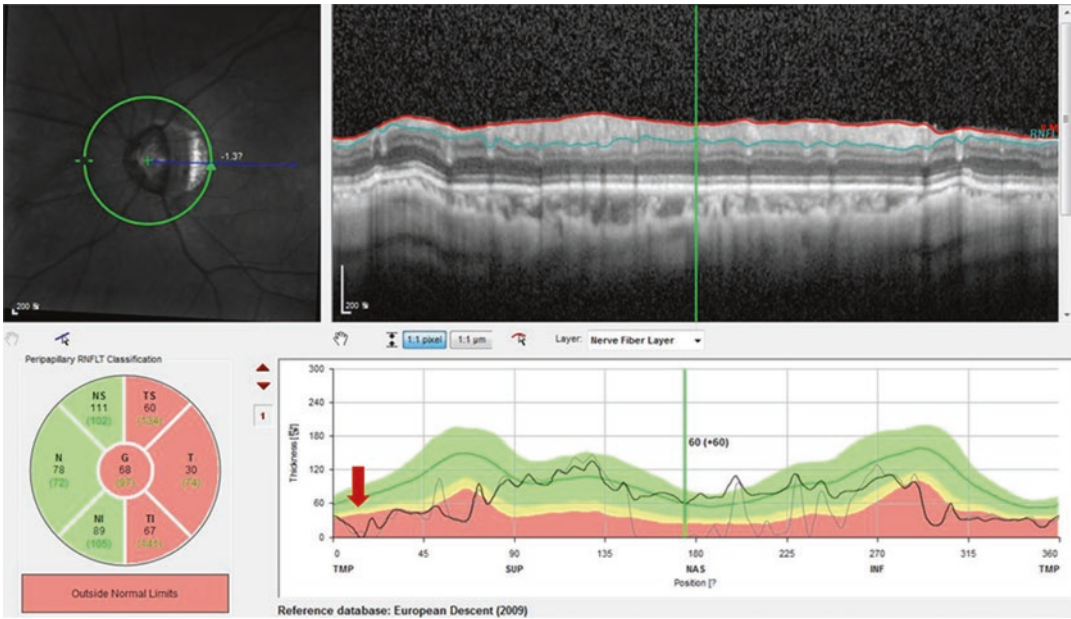


Fig. 3 Section seen to be passing through the area of peripapillary atrophy on careful examination of regions covered by peripapillary scanning ring (normally 3.46 mm in diameter). The segmentation error resulted from the

passage of the scanning ring over an atrophic area in the temporal quadrant. The values on the TSNIT profile are zero in that area (red arrow)

domain OCT (TD-OCT), due to the inability of the segmentation software to accurately align and register the A scans along the retinal pigmented epithelial border, which adversely affects segmentation of the retinal layers (Kim et al. 2012). Fortunately, with the advent of the newer SD-OCT, the inaccuracy of segmentation caused by peripapillary atrophy with TD-OCT is markedly reduced. Also, along with the presence of peripapillary staphyloma, there can be localized RNFL thinning depending on the size of the lesion (Fig. 4).

3.4 Media Opacity

Media opacities (e.g., dry eye, corneal opacity, cataract, and vitreous opacity) are the most common cause of artifacts in elderly patients (Fig. 5). They reduce signal strength and compromise retinal layer segmentation (Cheung et al. 2008; Vizzeri et al. 2009). In healthy patients analyzed with Stratus OCT, a positive linear relationship between signal strength and

mean RNFL thickness has been reported. It was found that for each unit of decrease in signal strength, the average RNFL thickness had a corresponding decrease of 2 μm (Vizzeri et al. 2009). Also, in the Cirrus platform, once the signal strength drops below a value of 7, the segmentation algorithm can sometimes fail and produce large regional errors in the derived RNFL thickness. Other OCT platforms have similar signal strength measurements.

The presence of vitreous opacities in the scanning area can cause imaging artifacts, often leading to red disease and sometimes to green disease. It can also cause the device to incorrectly detect the disc center, resulting in scanning of the wrong area. Focal media opacities, such as posterior vitreous detachment and hemorrhage, can cause a focal loss of signal strength, giving a false appearance of local areas of RNFL drop out that can lower the average RNFL thickness or artificially create segmental areas of thinning. Careful inspection of the RNFL thickness map, the deviation map, and the TSNIT graph can help clinicians identify this type of artifact.

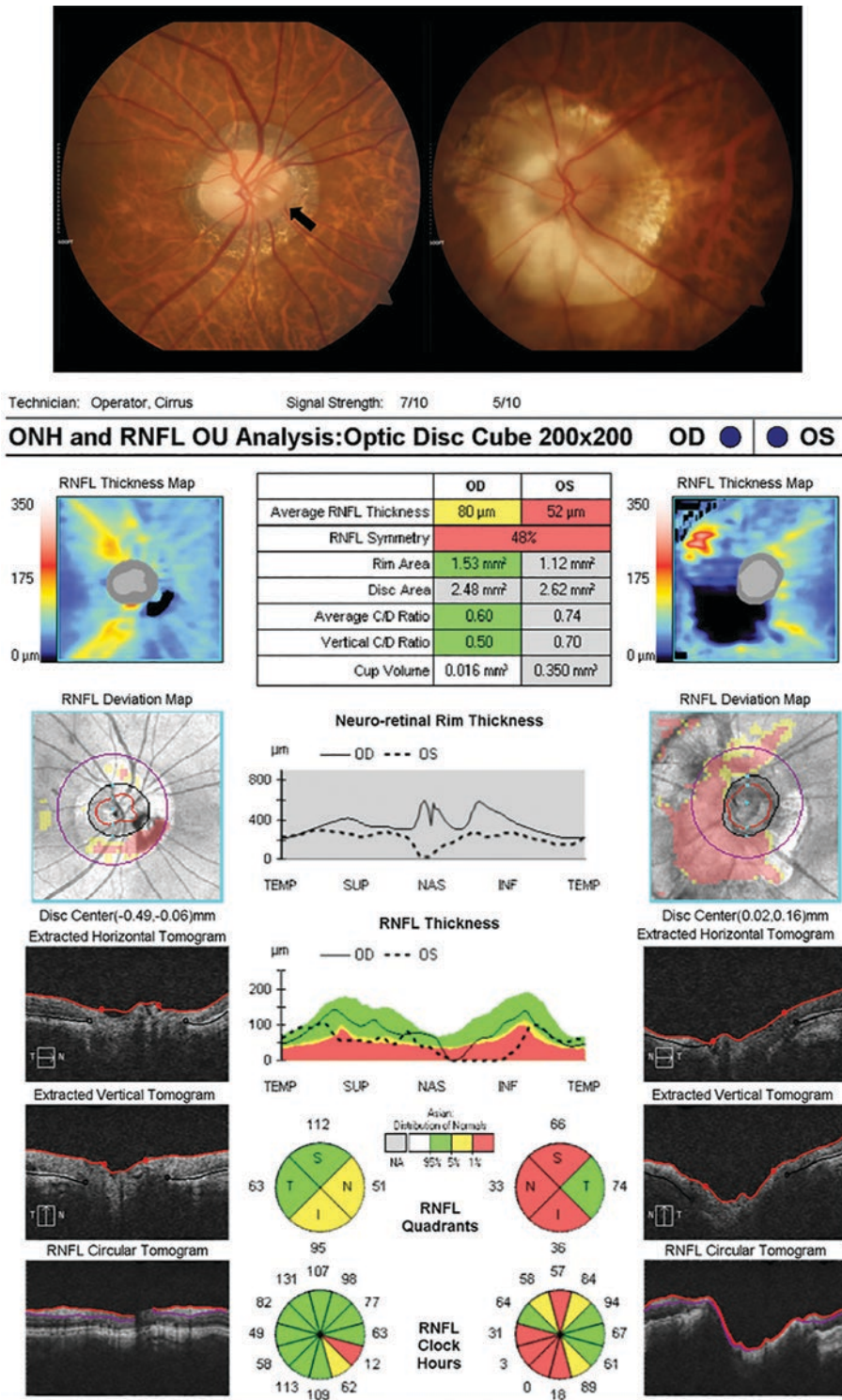


Fig. 4 Peripapillary staphyloma apparent in the left eye. The values on the TSNIT profile are zero in the region with segmentation error. The position of the Weiss ring in the right eye coincides with the RNFL calculation circle in

the inferior quadrant in the right eye (black arrow). In cases where the Weiss ring blocks part of the calculation circle, it can affect the TSNIT graph and all of the pie charts

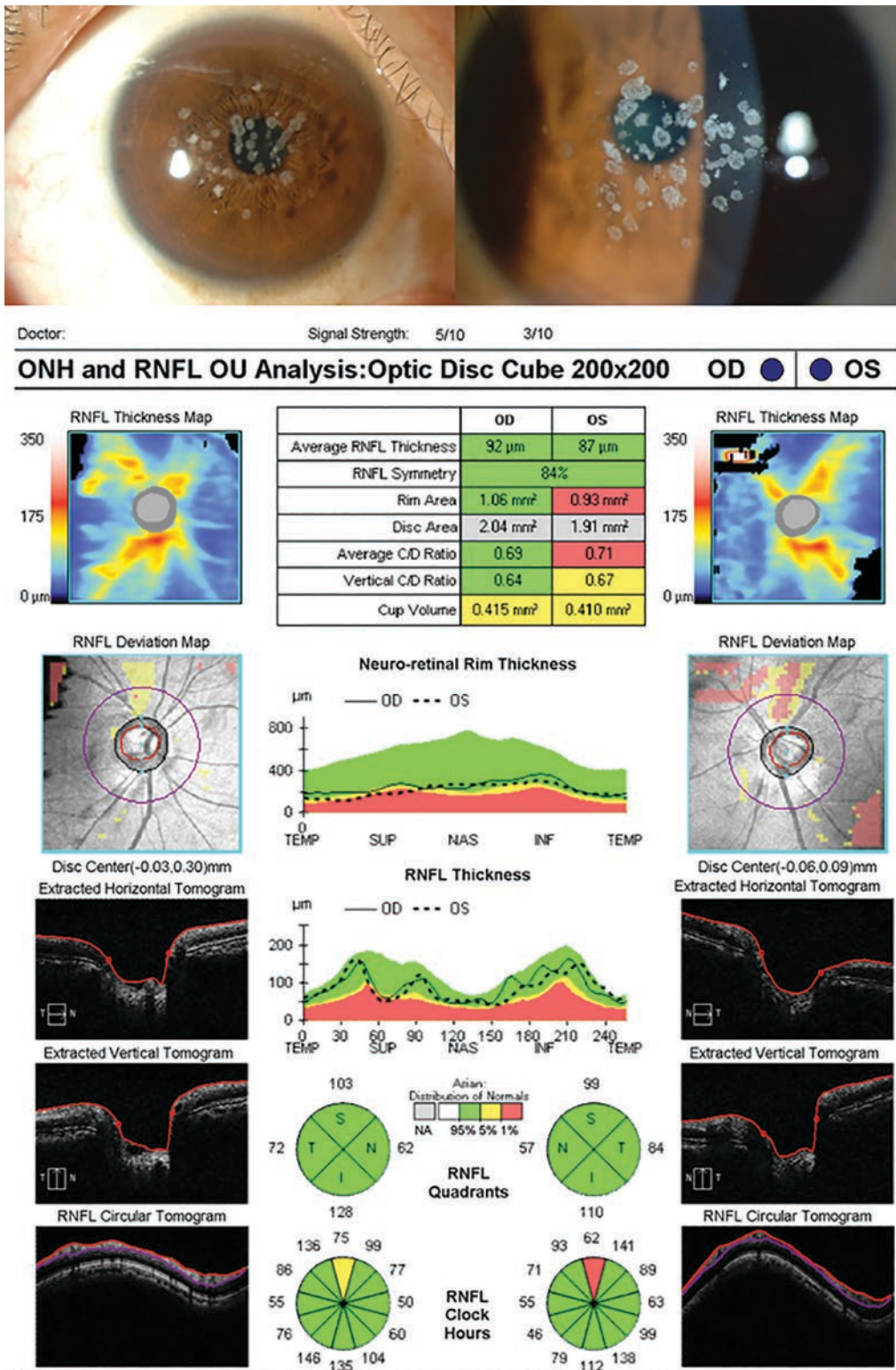


Fig. 5 OCT scan with low signal strength and multiple artifacts for both eyes diagnosed with Avellino corneal dystrophy. Note that the signal strength is 5 on the right

and 3 on the left. The interpreter needs to recognize this kind of artifact on the RNFL thickness map as an area of scanning failure or block

3.4.1 Dry Eye and Cataract

Glaucoma, dry eye, and cataract frequently coexist, due to their prevalence in aging populations (Congdon et al. 2004; Weinreb et al. 2014). In addition, ocular surface diseases such as dry eye syndrome are common in patients using topical ocular hypotensive drugs (Anwar et al. 2013). OCT studies have shown that these diminish the scan quality index and decrease RNFL thickness measures (Stein et al. 2006; Mwanza et al. 2011; Bambo et al. 2014). Patients are commonly instructed not to blink during camera alignment and scan acquisition; however, this may cause tear film evaporation and breakup, particularly in patients with preexisting ocular surface disorders. Patients should be encouraged to blink a few times immediately before scan capture to ensure uniform tear film distribution and to preserve adequate scan quality. This may also improve patient comfort, thus decreasing the likelihood of blink or motion artifacts during scan acquisition.

Cataracts are one of the most common causes of low-quality scans (Fig. 6). To obtain acceptable image quality, fine adjustments of the camera alignment may be attempted to purposely redirect the light beam through the areas of least opacity. Unfortunately, the detrimental effects of cataracts on OCT scan quality are difficult to overcome, unless cataract surgery is performed (Mwanza et al. 2011; Savini et al. 2006). Multifocal lenses may affect the quality of the OCT scan, leading to wavy horizontal artifacts (Inoue et al. 2009). How these artifacts affect RNFL measurements remains to be seen, but nonetheless, it is an important factor to consider as increasing numbers of patients receive multifocal lens implants.

3.4.2 Weiss Ring

Floating vitreous opacities, most commonly such as Weiss rings, can manifest and disappear on different scans as their position changes with eye movements. As the Weiss ring moves in front of the retina, it blocks the OCT signal in different areas of the optic nerve head or retina on different scans (Fig. 4). It can cause red disease artifacts,

even when not overlying the calculation circle. Additionally, it may cause green disease artifacts located over the optic nerve.

3.5 Vitreoretinal Interface Problems

A prominent vitreoretinal interface opacity can cause errors in the segmentation of RNFL thickness. OCT algorithms attempt to identify the internal limiting membrane as the upper boundary of the RNFL. Occasionally a prominent vitreous opacity will be incorrectly identified as the internal limiting membrane, which will result in an artifactually thickened RNFL measurement.

3.5.1 Peripapillary Vitreoretinal Traction

Vitreoretinal traction can result in an artificially high increase of RNFL thickness and may lead thereby to green disease artifact. This situation can occur when posterior vitreous detachment is developing or be due to posterior hyaloid thickening. Segmentation errors may also occur as the results of the presented average RNFL thickness values being much higher than expected (Figs. 7 and 8). Unless details of the vitreous interface with the internal limiting membrane are visible, a potential area of artifact could easily be overlooked. If the vitreous completely separates from the retina, RNFL thickness may decrease significantly and reveal the actual extent of RNFL loss. Clinicians should be careful not to interpret the reduction of RNFL thickness upon release of vitreoretinal traction as structural glaucoma progression.

3.5.2 Epiretinal Membrane

Epiretinal membrane can also cause artificially high RNFL thickness measurements and result in green disease (Asrani et al. 2014). The software algorithm identifies the upper boundary of the epiretinal membrane as that of the upper edge of the RNFL or as the internal limiting membrane of the retina, leading to erroneous measurements (Figs. 8 and 9). It is easily visible with SD-OCT machines that show the details of the vitreous-

b

Technician: Operator, Cirrus

Signal Strength: 7/10

7/10

ONH and RNFL OU Analysis: Optic Disc Cube 200x200 OD ● ● OS

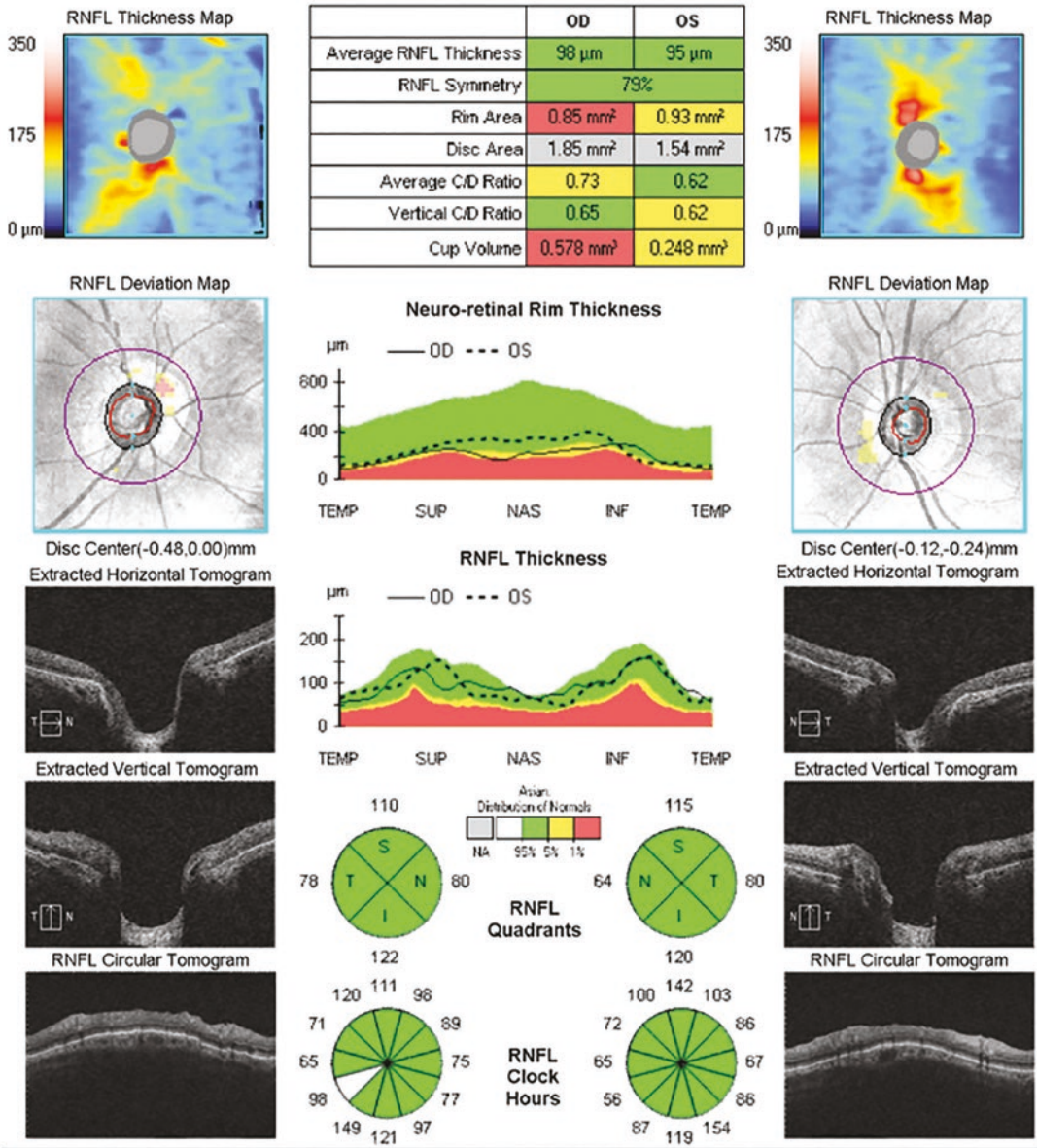


Fig. 6 (continued)

internal limiting membrane interface. The presence of an epiretinal membrane in a macular thickness scan should alert the physician to the possibility of an artifact on the RNFL scan.

3.5.3 Peripapillary Retinoschisis

Peripapillary retinoschisis is characterized by splitting of the peripapillary RNFL. It has been described in patients with different types of

a

High Definition Images: HD 5 Line Raster

OD OS

Scan Angle: 0°

Spacing: 0.25 mm

Length: 6 mm

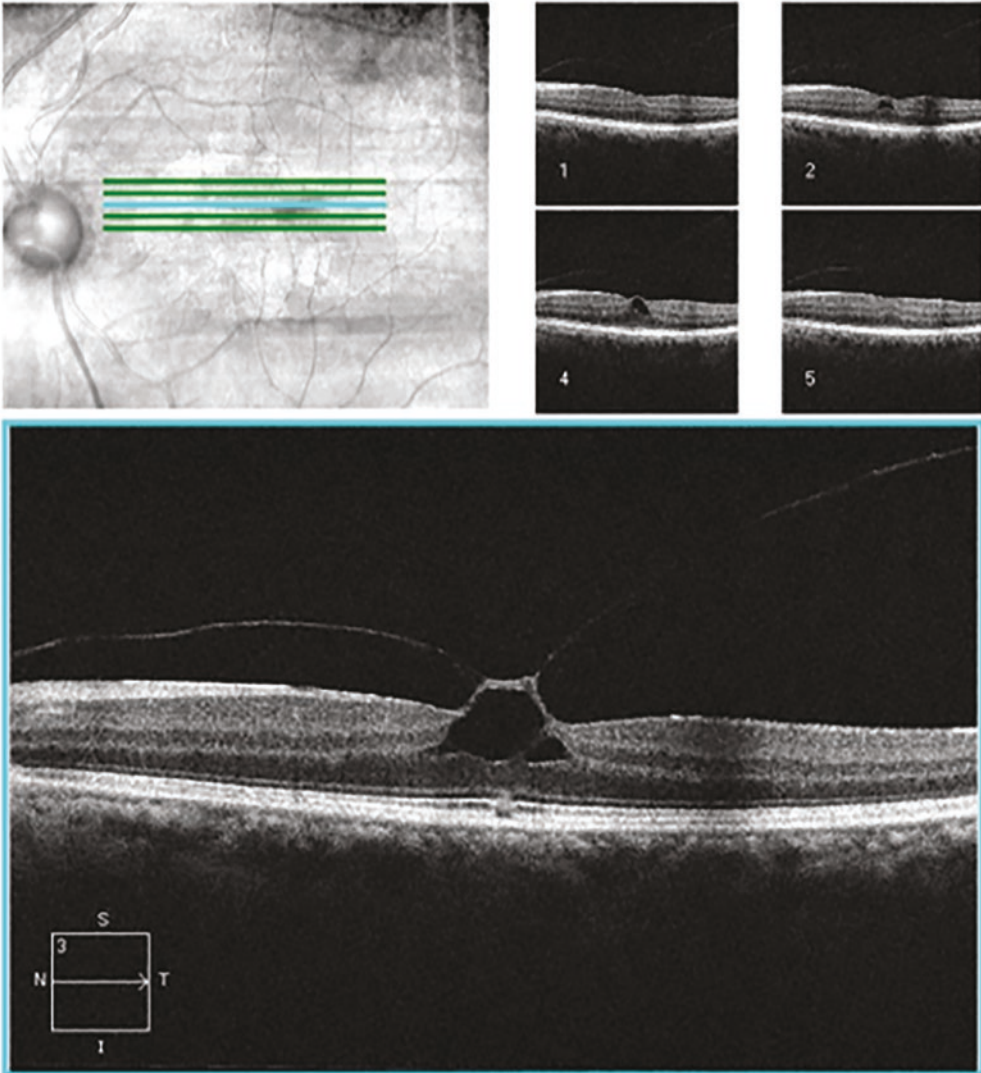


Fig. 7 (a) Cirrus HD-OCT demonstrating vitreoretinal traction in the left eye. (b) Areas of vitreous RNFL adhesions lead to tractions and artificial thickening of RNFL on the RNFL thickness map (red arrows)

b

Technician: Operator, Cirrus

Signal Strength: 9/10

8/10

ONH and RNFL OU Analysis: Optic Disc Cube 200x200 OD ● ● OS

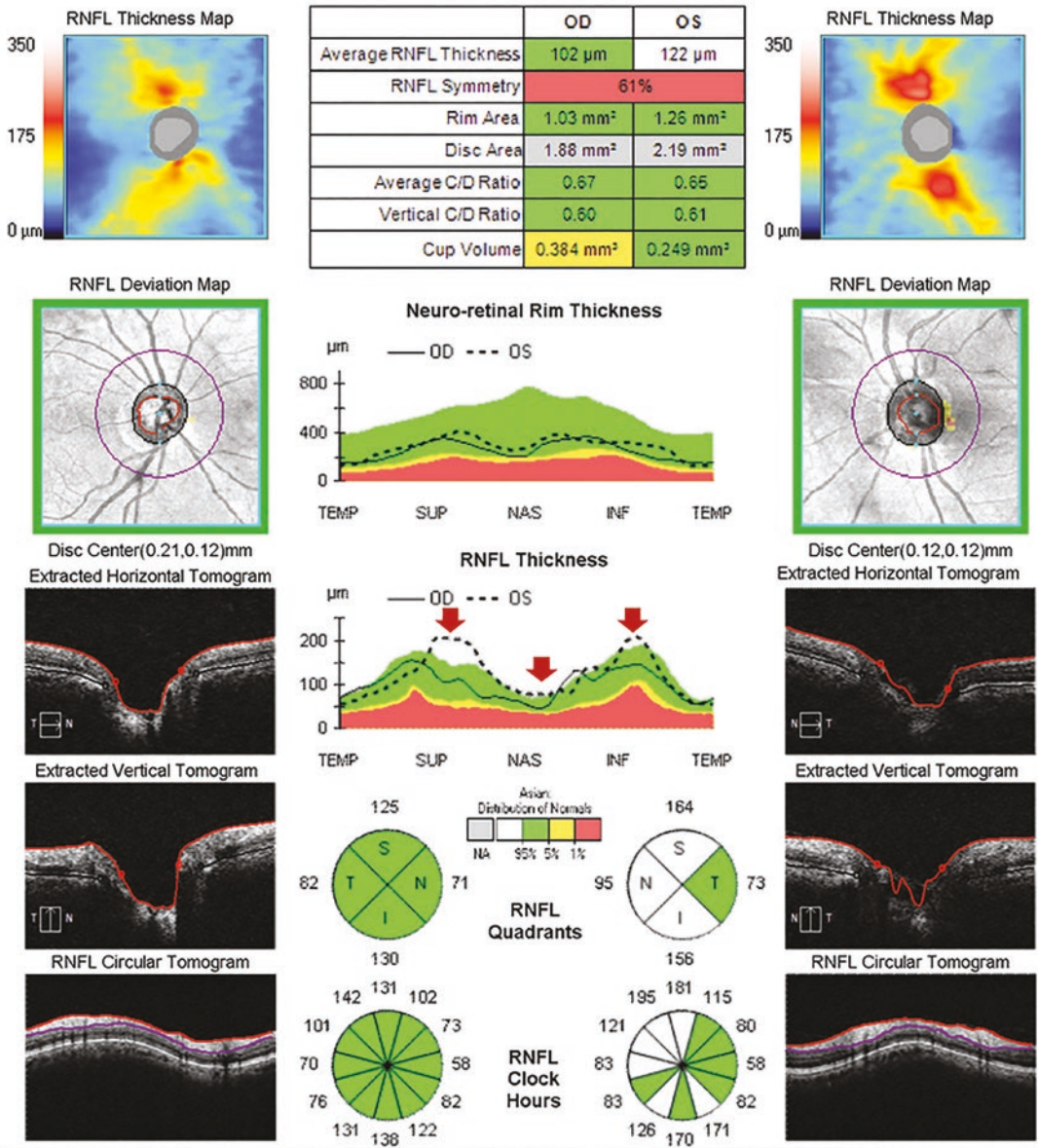


Fig. 7 (continued)

glaucoma, including primary open-angle glaucoma, angle-closure glaucoma, and pseudoexfoliation glaucoma (Zhao and Li 2011; Hollander et al. 2005; Kahook et al. 2007; Örnek et al. 2013). Temporary increase in RNFL thickness

measurements is found in eyes with peripapillary retinoschisis, and after resolution of the retinoschisis, RNFL thickness may decrease remarkably (Hwang et al. 2014; Bayraktar et al. 2016) (Fig. 10). If a clinician simply looks at the mea-

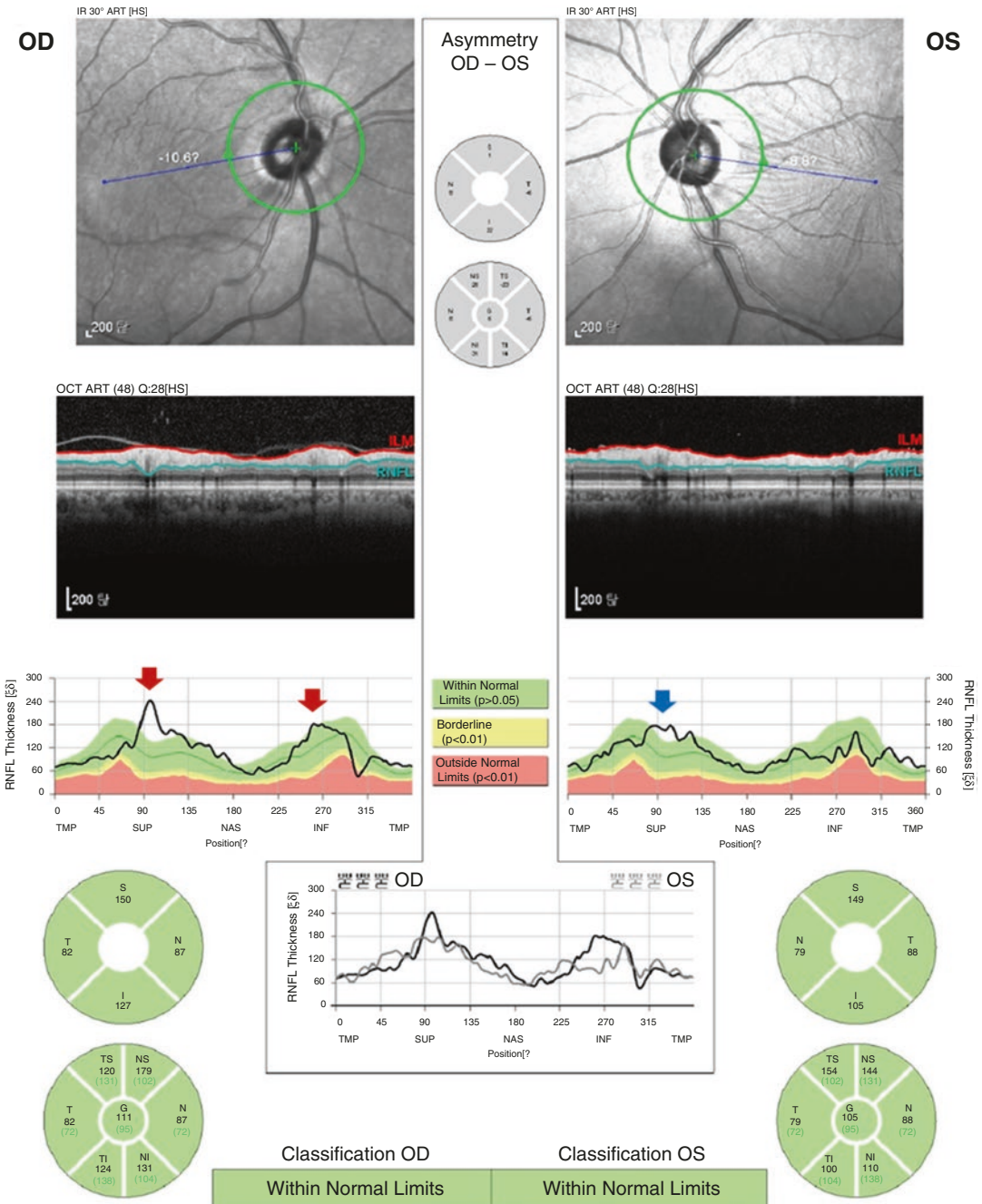


Fig. 8 Spectralis OCT demonstrating vitreoretinal traction in the right eye and epiretinal membrane in the left eye. In the right eye, the areas of vitreous RNFL adhesions lead to tractions and artificial thickening of the

RNFL (red arrows). In the left eye, the software algorithm has misidentified the boundary of the epiretinal membrane as the upper edge of the RNFL, leading to an erroneously elevated RNFL measure in that region (blue arrow)

surement data without noticing the retinoschisis, such a decrease may be considered to be a rapid progression of glaucoma. Clinicians should examine thickness maps as well as horizontal

B-scans in order to detect retinoschisis, so as not to overestimate RNFL thickness or misinterpret the resolution of retinoschisis as rapid structural progression.

3.5.4 Edema of Retina

Edema of the retina can have a large effect on the signal strength of the layers under it and, thus too, on the accuracy of segmentation by OCT. Green disease may appear in the form of thinning in certain sectors in eyes with very high RNFL thickness values. In diabetic macular edema, RNFL thickness measurements may be high due to the retinal edema, despite the fact that the presence of glaucomatous damage and green classification in these sectors may obscure the glaucomatous damage (Fig. 11). Also, edema caused by uveitis or age-related macular degeneration may mask glaucomatous RNFL thinning, thus leading to green disease (Moore et al. 2015). In peripapillary retinoschisis, there is a temporary increase in RNFL thickness, the values

returning to normal after its resolution (Bayraktar et al. 2016; Hwang et al. 2011).

3.6 Optic Nerve Head Pathologies

In addition to the aforementioned diseases, optic nerve head pathologies can make segmentation inaccurate in the RNFL thickness plot and optic nerve head. Failed segmentation can often be identified as an area of absolute loss in the Cirrus RNFL deviation map that does not follow the normal arcuate pathway of the RNFL. Errors in segmentation can also be seen by examining the TSNIT RNFL thickness plot, which is available on most commercially available OCT displays (Fig. 12). Also, the segmentation algorithm may report a disc area

a

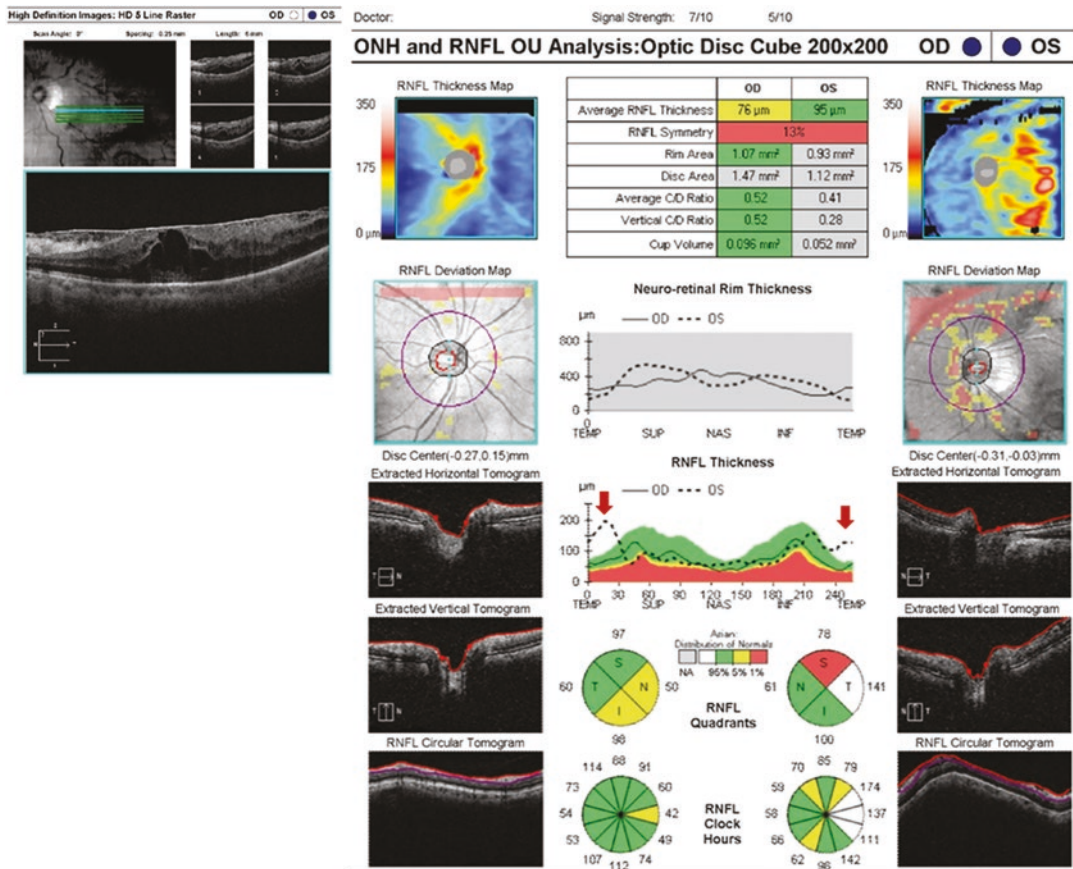


Fig. 9 (a) Cirrus HD-OCT demonstrating epiretinal membrane in the left eye. Multiple segmentation errors are present and the thickness of the RNFL in the temporal quadrant is increased. This was most likely caused by the

traction forces on the retina. **(b)** Cirrus HD-OCT of the same patient after epiretinal membrane removal surgery. The RNFL thickness of the temporal quadrant is within normal range

b

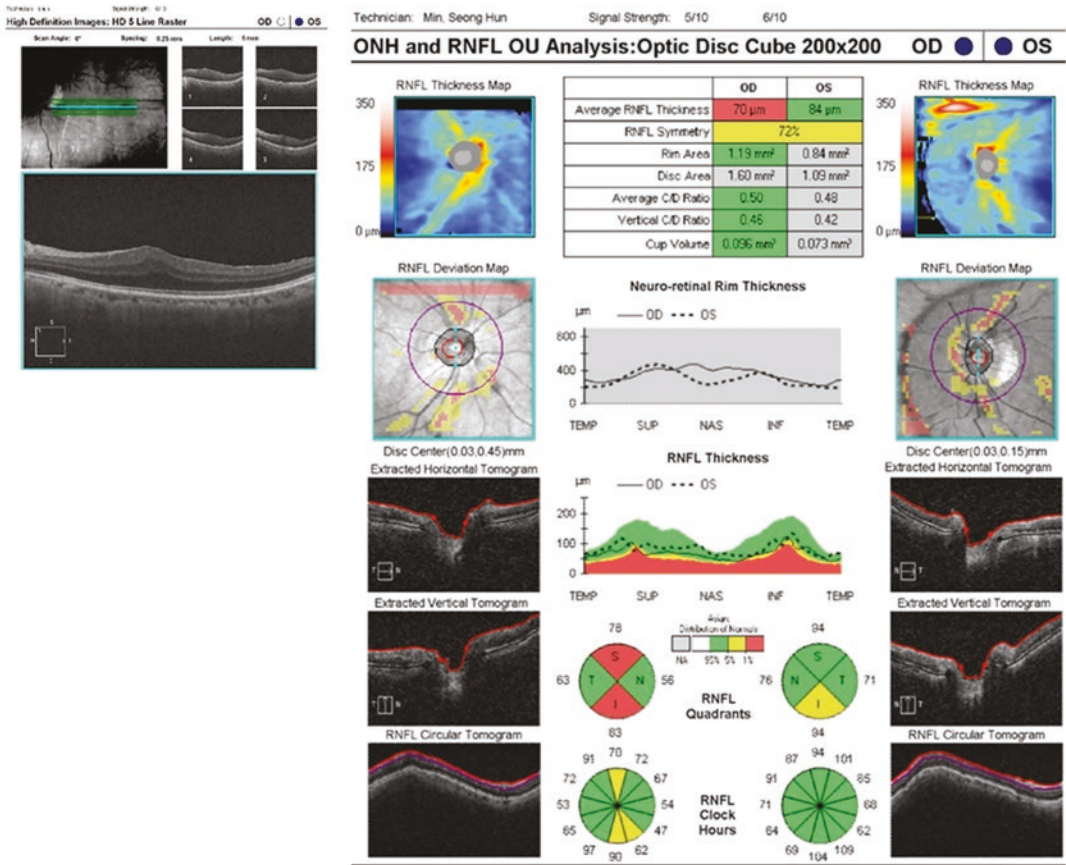


Fig. 9 (continued)

larger than its true size because the termination point of the Bruch’s membrane and its termination at the neural canal opening are inaccurately located more proximally (Chen and Kardon 2016). In the case of an oversized optic nerve head, the peripapillary RNFL scanning ring will pass close to the disc margin, leading to inaccurate results (Bayer and Akman 2020). Errors in the determination of the border of the neural canal (disc area) will adversely affect the determination of the location and area of the rim as well as the cup-to-disc ratio.

In optic nerve head drusen, the cup area or volume is very small or at a value near zero despite a normal disc size. Also, neuroretinal rim thickness above the normal values is conspicuous. The presence of a myelinated nerve fiber layer can also lead to an increase in RNFL thickness that can lead in turn to overestimation of the number of axons in the corresponding location. Thickly myelinated nerve fibers can hide glaucomatous

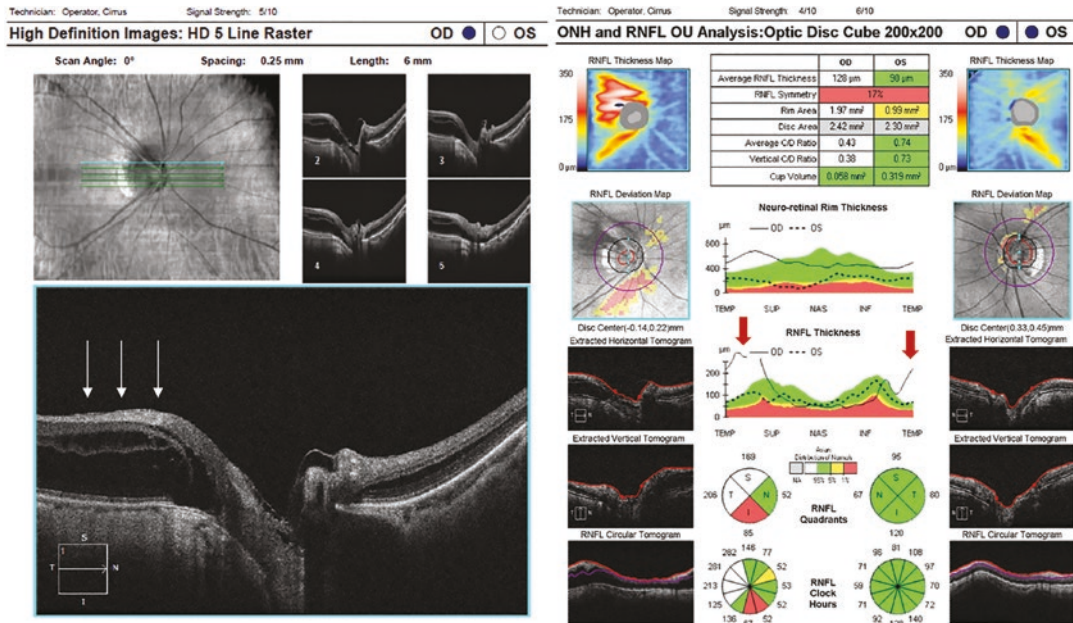
RNFL loss and may cause inaccurate segmentation and green disease. Again, in such cases, the peripapillary scan should be repeated with a larger ring diameter, or alternatively, macular and optic nerve head analyses should be performed.

In eyes with optic nerve head pathologies, it can be very difficult to isolate the glaucomatous damage by structural or functional tests. Progression analysis can be beneficial if there is suspicion or diagnosis of glaucoma; however, it should be noted that optic nerve head pathologies such as optic disc drusen itself may also cause progressive RNFL and visual field losses in a manner similar to glaucoma (Savino et al. 1979; Roh et al. 1998).

3.7 Pupil Size

Small pupil size may potentially reduce the amount and quality of the signal detected by

a



b

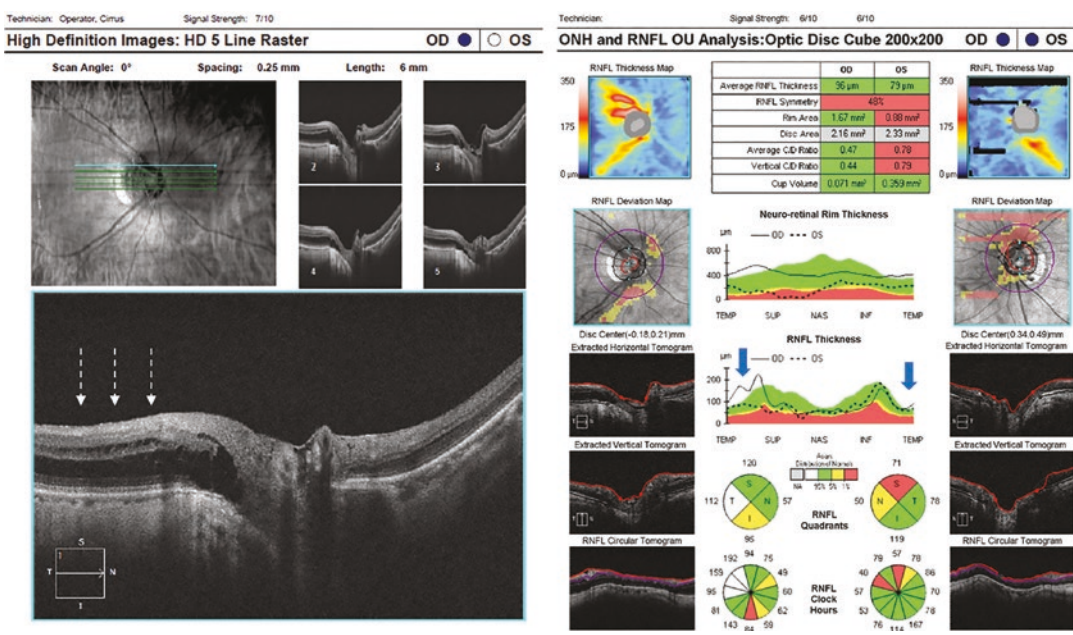


Fig. 10 (a) Peripapillary retinoschisis observed in the right eye (white arrows). The RNFL thickness curve is well above the expected values in the location corresponding to the region of retinoschisis. **(b)** Two years later, the extension of retinoschisis has become smaller (white dot-

ted arrows). A remarkable decrease in the RNFL thickness in the superior and temporal areas also can be seen (blue arrows). **(c)** Guided progression analysis map showing progressive RNFL loss that can be misinterpreted as structural progression of glaucoma

C

Guided Progression Analysis: (GPA™)

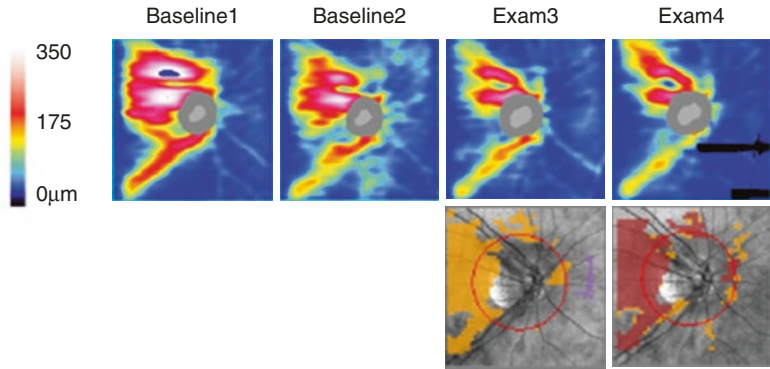


Fig. 10 (continued)

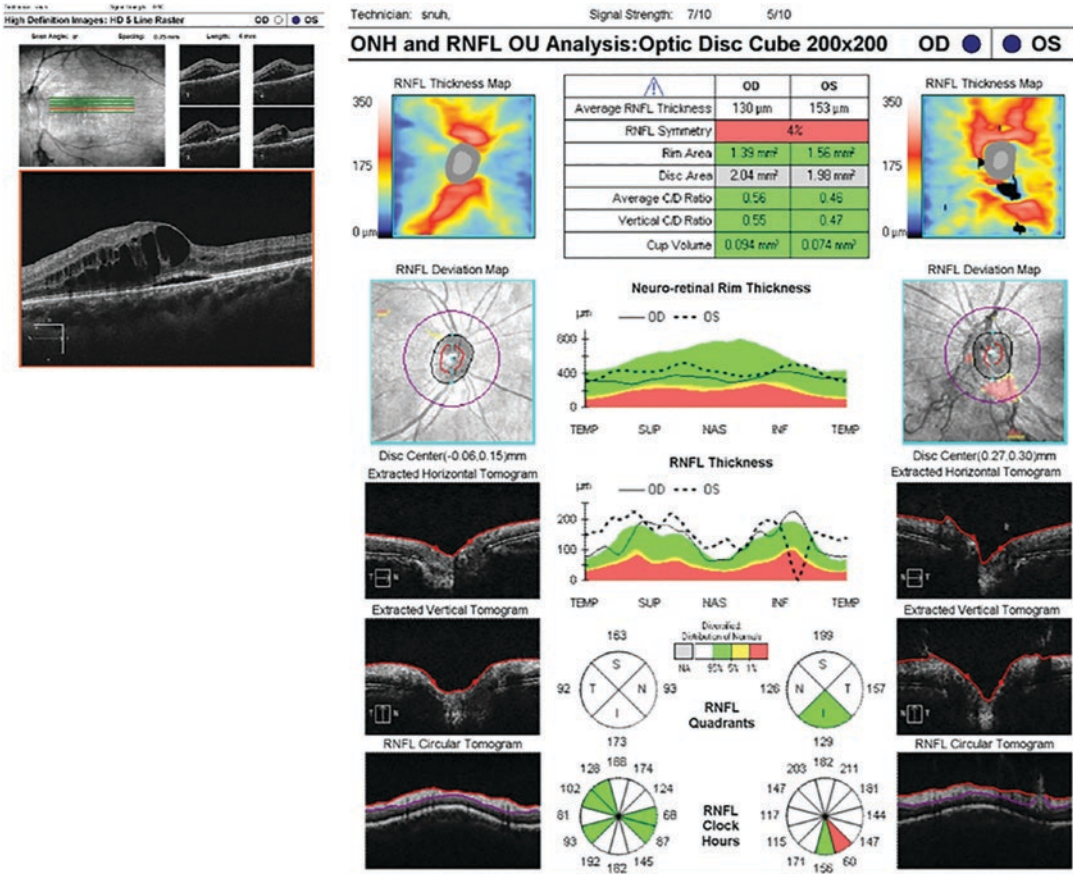


Fig. 11 Cirrus HD-OCT showing a patient with diabetic retinopathy and macular edema. In the TSNIT profile, the thickness curve is seen to be above normal limits. The optic nerve head parameters are within normal range, pos-

sibly due to the adhesions between the vitreous and the optic disc. In the inferotemporal area with peripapillary vitreoretinal traction, note the segmentation resulting in the RNFL thickness of zero

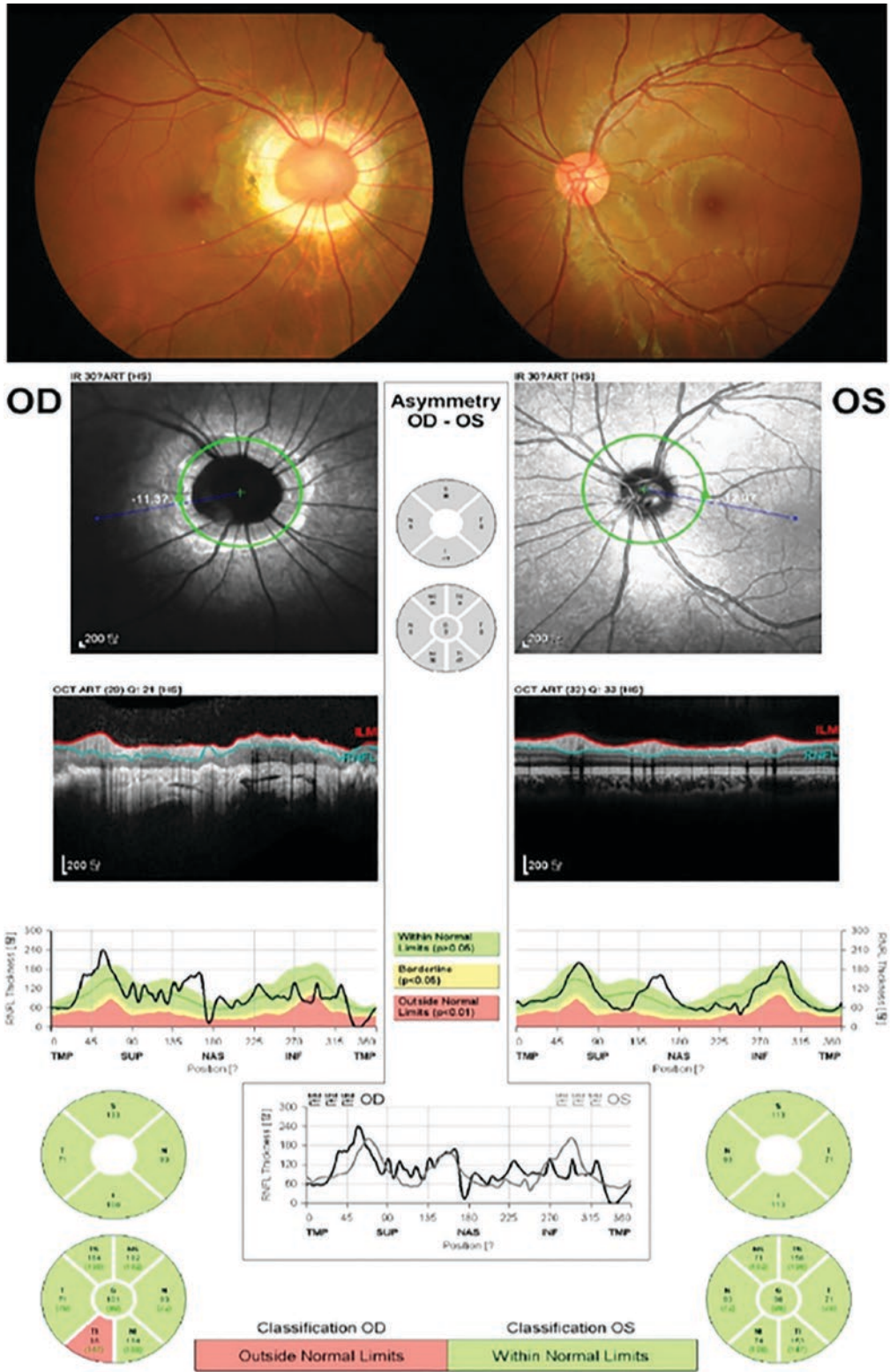


Fig. 12 Morning glory syndrome in the right eye causing segmentation artifact. On the TSNIT profile, it is seen that RNFL thickness has a value near 0 in the nasal quadrant and 0 in the temporal quadrant

a

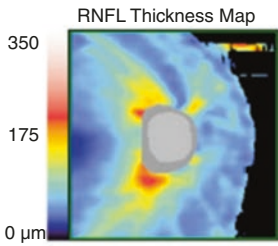
Doctor:

Signal Strength: 6/10

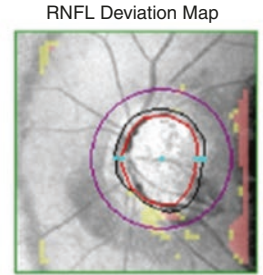
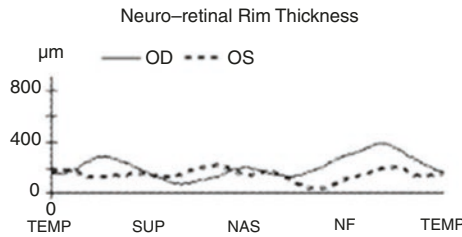
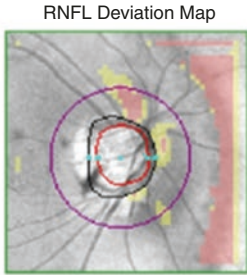
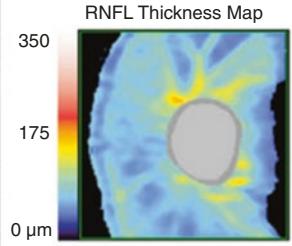
5/10

RNFL and ONH:Optic Disc Cube 200x200

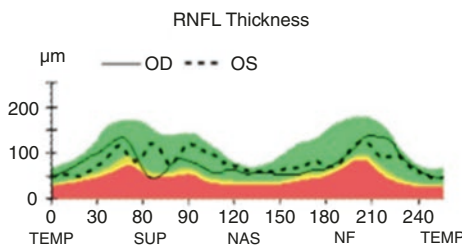
OD ● OS



	OD	OS
Average RNFL Thickness	80 μm	83μm
RNFL Symmetry	56%	
Rim Area	1.15 mm ²	1.08 mm ²
Disc Area	2.85 mm ²	4.67 mm ²
Average C/D Ratio	0.75	0.86
Vertical C/D Ratio	0.73	0.89
Cup Volume	0.551 mm ³	1.400 mm ³



Disc Center(-0.18,-0.12)mm
Extracted Horizontal Tomogram



Disc Center(0.60,-0.15)mm
Extracted Horizontal Tomogram

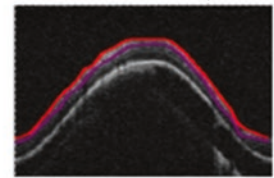
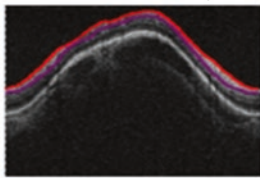
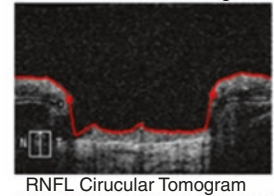
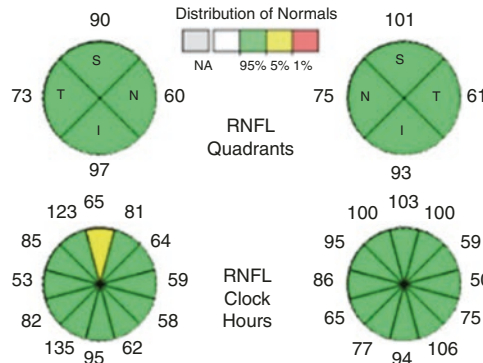
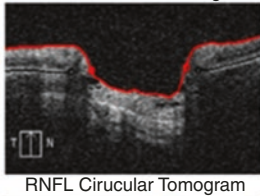
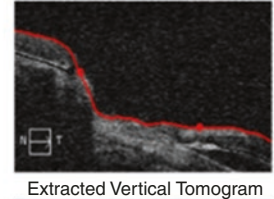
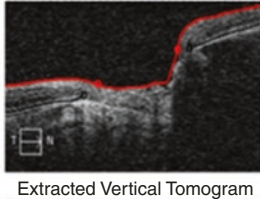


Fig. 13 (a) Borderline-quality Cirrus HD-OCT scan with signal strength of 6 in the right eye and 5 in the left eye of a small-pupil patient. Small pupil may have reduced the amount and quality of the signal detected by the instru-

ment. **(b)** Cataract formation in both eyes of the same small-pupil patient. The coexisting cataract diminished the scan quality (signal strength, both eyes: 3) and decreased the RNFL thickness measures

b

Technician: Operator, Cirrus

Signal Strength: 3/10

3/10

ONH and RNFL OU Analysis: Optic Disc Cube 200x200 **OD** ● ● **OS**

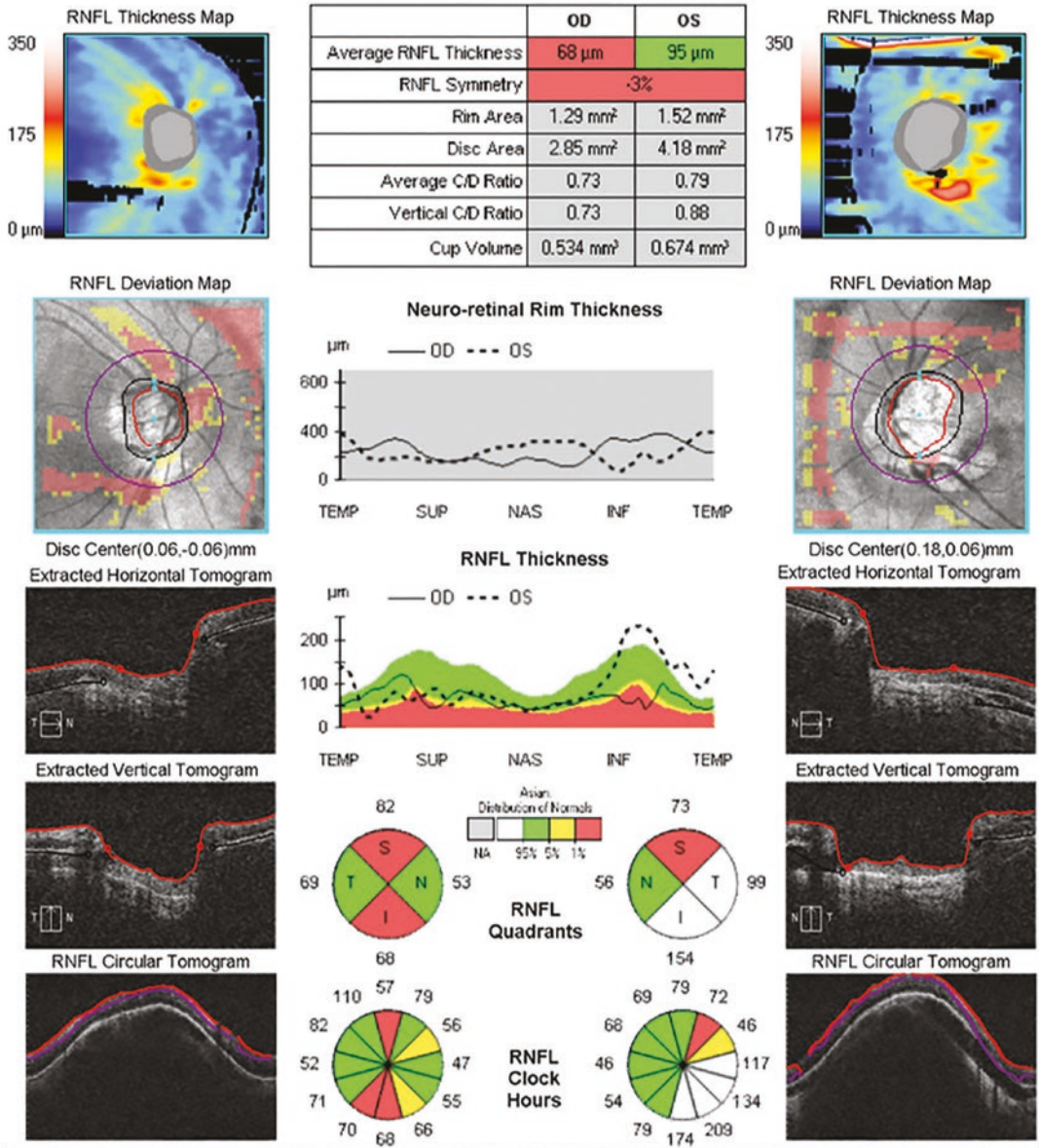


Fig. 13 (continued)

OCT (Fig. 13). Scans can be obtained in eyes with a pupil diameter greater than 2 mm. Recent studies have not found significant changes in RNFL thickness before and/or after dilation,

which suggests that the effect of pupil size is insignificant (Massa et al. 2010; Savini et al. 2010). However, pharmacological dilation may be necessary in selected cases of small pupil size.

3.8 Motion Artifact

Motion artifact results from eye movements (e.g., horizontal saccades) during scan acquisition. Improvements in SD-OCT scanning speed and acquisition time have reduced the likelihood of motion artifact. However, for devices lacking an eye-tracking system or motion correction algorithms, eye movements remain a potential problem. Careful interpretation of results, including retinal vessels, optic disc shape, and clock-hour RNFL thickness, is warranted in scans with motion artifacts passing through the optic disc (Taibbi et al. 2014). Patients' steady fixation is required to avoid motion artifacts. It may be noticed during scanning that the disc or macula is not well centered. In such cases, a clear explanation of the scanning procedures and timely notification to the patient of imminent image acquisition may be helpful. Rescans should be attempted, and if necessary, an external fixation point can be used.

3.9 Blink Artifact

Although image acquisition time is less than 2 s, blinking may yet occur during this time frame. The effects of blink artifact on OCT depend on its position within the scan area (Fig. 14). In the absence of an eye-tracking system, the acquisition process continues even in the presence of blinking. This leads to transient loss of data, which is proportional to the duration of a single blink. Blink artifacts can be prevented by allowing the examinee to blink freely until the completion of the camera alignment process, followed by prompt notification of the imminent start of scan acquisition. In selected cases, artificial tears or other lubricants may be useful.

4 Instrument Factors

4.1 Poor Image Quality

A good-quality scan is essential for a reliable OCT result. All OCT devices use quality-control sys-

tems for assessing image quality. The "strength" of the light signal backscattered by the ocular structures, calculated as the signal-to-noise ratio, has been conventionally used as an objective measure of scan quality. Cirrus HD-OCT uses the "signal strength" parameter for this purpose and recommends a repeated scan if the signal strength is below 6. Spectralis OCT uses a quality score, or the "Q" coefficient, for the same purpose; values less than 20 require repetition of the test. Poor signal strength has been demonstrated as a major source of artifacts in previous studies as well and precludes the ability to detect change in the RNFL overtime (Vizzeri et al. 2009; Wu et al. 2007). Poor scanning quality can lead to inaccurate RNFL thickness measurements, specifically thinner-than-actual values (Rao et al. 2014; Huang et al. 2011; Russell et al. 2014). Several ocular-related factors may play a role in OCT scan quality, as outlined above (Stein et al. 2006; Mwanza et al. 2011; Bambo et al. 2014; Savini et al. 2010). In addition, operator-dependent factors, such as improper OCT lens cleaning or poor image centration, may affect results.

4.2 Poor OCT Device Performance

As an OCT device gets older and undergoes heavy use, the power of the superluminescent-light-emitting diode decays over time, the optics become dirty, and images opaque. The result is poor-quality scans in almost all patients, especially those with early cataracts or dry eyes.

4.3 Inaccurate Optic Disc Margin Delineation

Adequate optic disc assessment relies on the ability of the automated algorithm to identify the termination of the Bruch's membrane corresponding to the optic disc edge (Strouthidis et al. 2009a, b). Accurate delineation of the optic disc margin is incorporated in the optic disc center location. In eyes with peripapillary atrophy, the OCT signal reflectance alters due to retinal pigment epithelium disruption and choriocapillaris atrophy

a

Signal Strength: 7/10 7/10

ONH and RNFL OU Analysis: Optic Disc Cube 200x200 OD ● OS ●

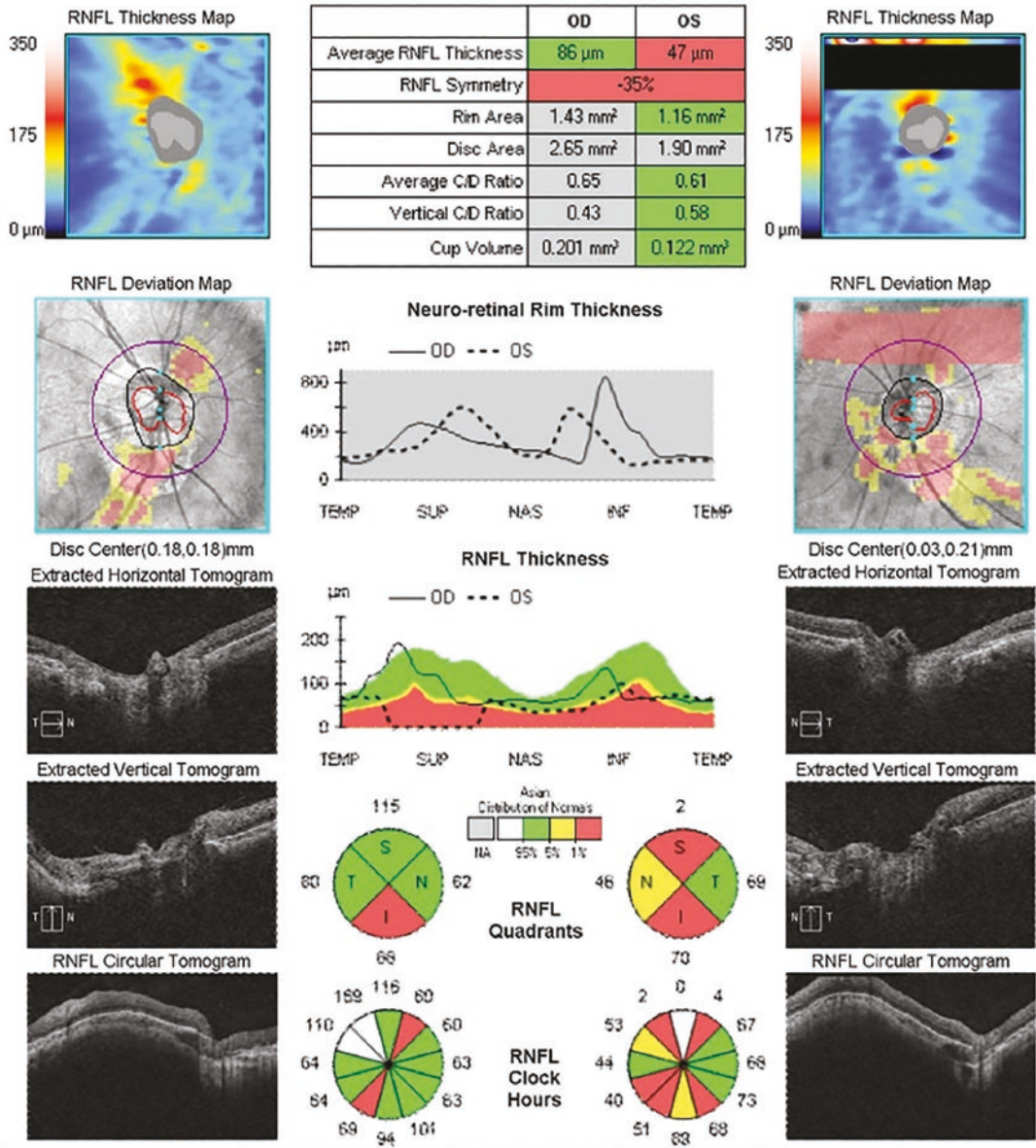


Fig. 14 (a) Blink artifact in the left eye. The blink produced a well-demarcated rectangular area of missing data and red superpixels spanning the entire width of the

RNFL thickness map. **(b)** Rescan of the same patient. The RNFL thickness of the superior quadrant in the right eye as measured was within the normal range

b

Technician: Operator, Cirrus

Signal Strength: 8/10

8/10

ONH and RNFL OU Analysis: Optic Disc Cube 200x200 OD ● ● OS

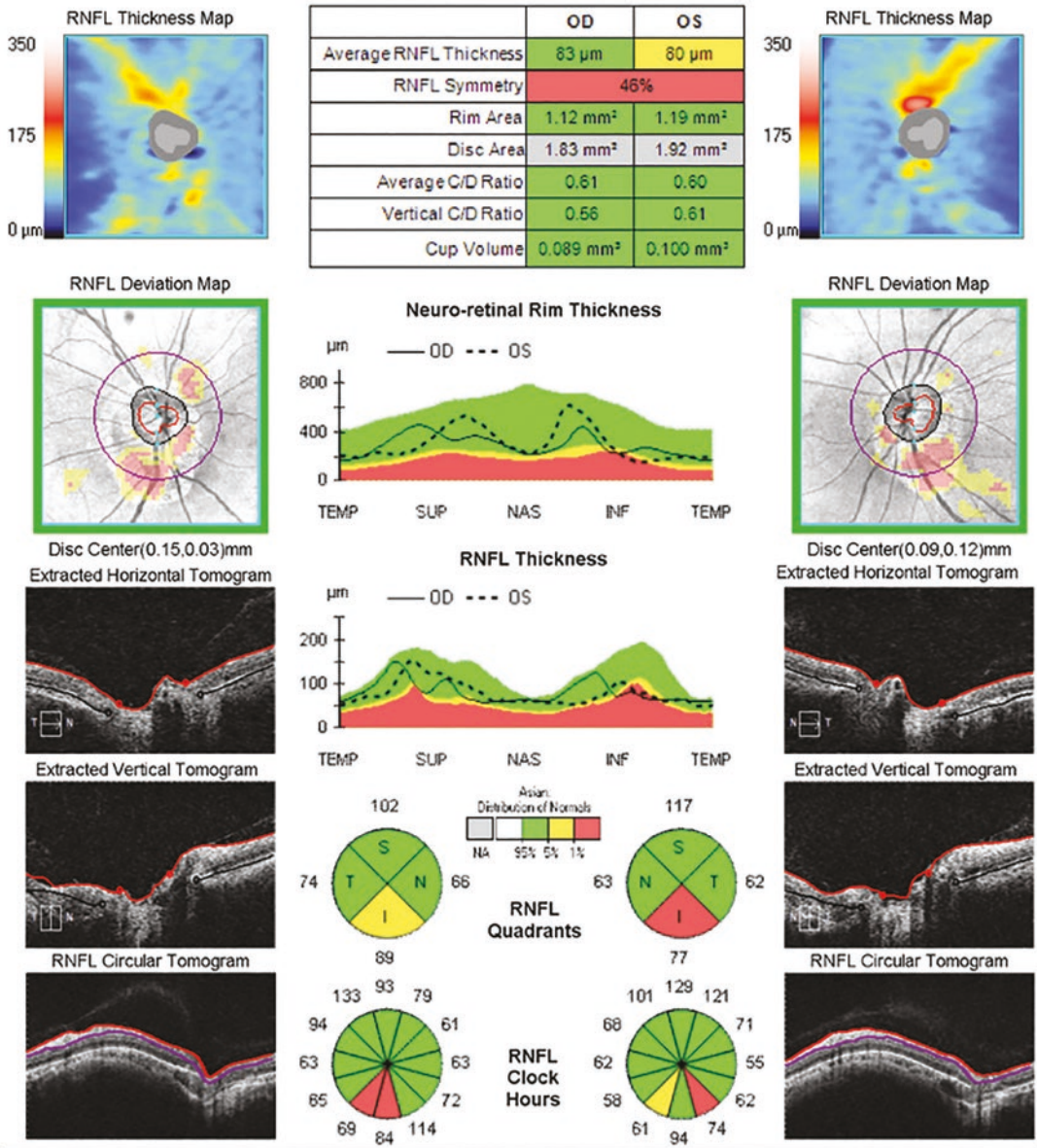


Fig. 14 (continued)

(Manjunath et al. 2011), coupled with Bruch’s membrane changes (Curcio et al. 2000). This possibly affects the identification of the optic disc margin (Fig. 15). Blinking or optic disc cup truncation may also lead to unreliable optic disc

parameters. Therefore, for each scan, careful inspection of the en-face image and the tomograms intersecting the optic disc is necessary. Moreover, rescans should be attempted in order to obtain accurate optic disc margin outlining.

Doctor:

Signal Strength: 9/10

7/10

ONH and RNFL OU Analysis: Optic Disc Cube 200x200

OD ● ● OS

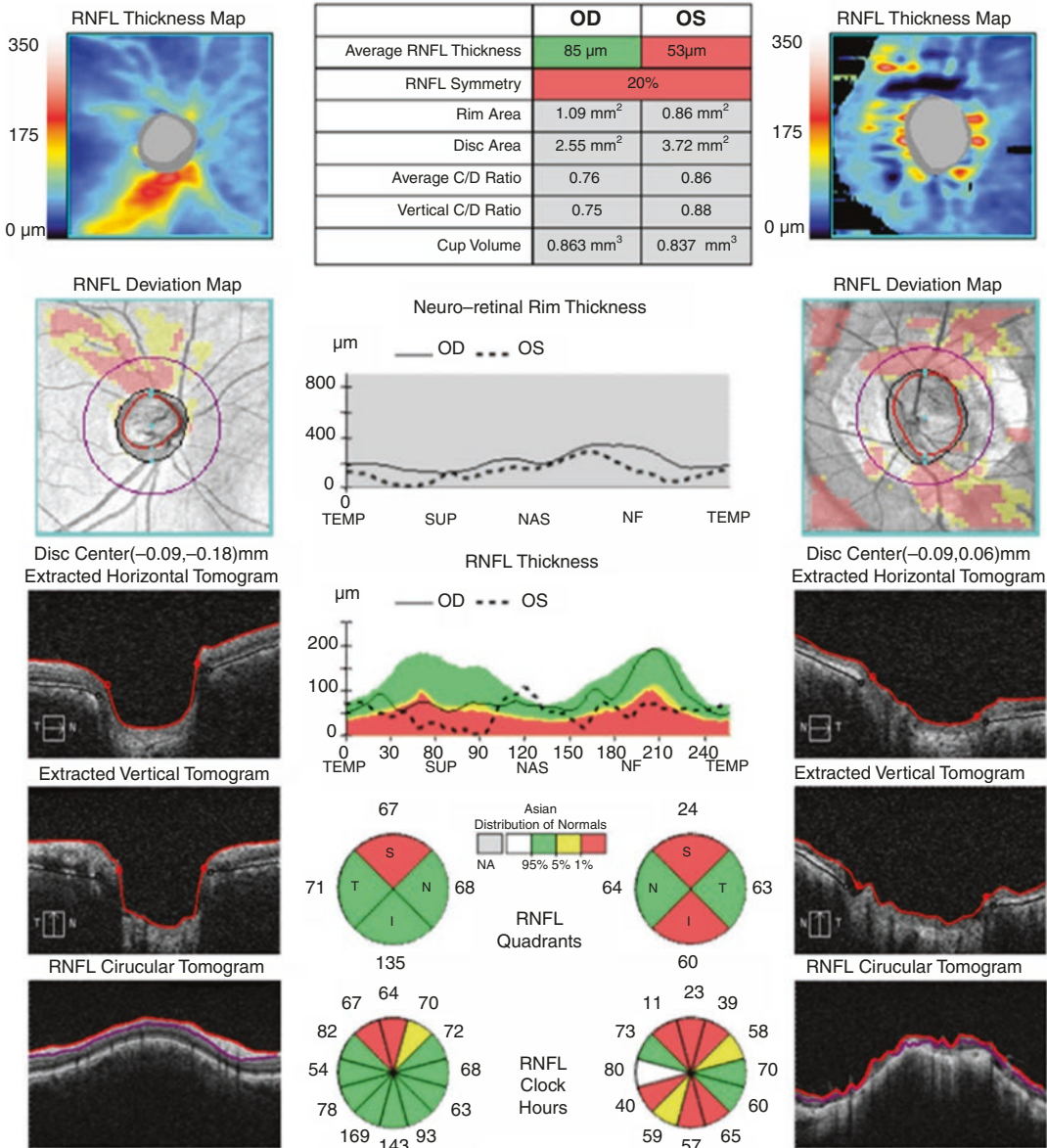


Fig. 15 Inaccurate optic disc margin delineation and segmentation artifact in Cirrus HD-OCT imaging of RNFL in a patient with large peripapillary atrophy in the left eye. The inaccurate delineation of the disc resulted in the arti-

facts of RNFL thickness. The RNFL thickness was measured as zero with large areas of abnormal thickness flagged as red areas

4.4 Segmentation Errors

All OCT devices have segmentation algorithms or layer-seeking algorithms to enable analysis and measure a target retinal layer. Segmentation errors

occur when the software is unable to determine the layers correctly. Several mechanisms may be responsible for inaccurate RNFL segmentation, such as OCT signal attenuation with decreased reflectance of the RNFL caused by media opaci-

ties. The OCT signal may be interrupted by the effects of blinking or floaters, causing localized failure to identify the RNFL boundaries and decreased RNFL thickness measures. Moreover, truncation of the inner retinal layers may determine algorithm failure or obvious RNFL segmentation errors. Finally, motion artifacts intersecting the scan circle may incur inaccurate RNFL segmentation. In such cases, the RNFL or other retinal layer being assessed is measured as thicker or, more commonly, thinner than it actually is. RNFL thickness could be measured as zero and flagged as a red area (Fig. 16). Very low measurement of RNFL thickness, usually thinner than 30 μm , is due mostly to segmentation or imaging error (Chan and Miller 2007; Groth et al. 2013).

5 Operator Factors

5.1 Registration Error of Age

Thickness measurements obtained from an OCT device are compared against age-matched controls in order to identify significant thinning or thicken-

ing. There is a natural attrition of the RNFL with aging (Budenz et al. 2007; Parikh et al. 2007). One study reported that the overall mean RNFL thickness on OCT decreases by 0.365 mm for every year increase in age (Celebi and Mirza 2013). Therefore, not accounting for age effects can significantly affect estimates of disease progression (Leung et al. 2013). Entering the incorrect date of birth could cause abnormalities in the probability plots of thickness measurements that could lead to erroneous interpretation.

5.2 OCT Lens Opacities

Opacities of the OCT lens may occur from fingerprints or the patient's accidental contact with the lens. They can decrease image quality and directly affect RNFL thickness measures. On the final printout, they typically maintain an identical shape and occupy the same position on the en-face image over repeated testing. Periodic lens cleaning coupled with careful handling of the device by test operators and patients is necessary to prevent the occurrence of such artifacts.

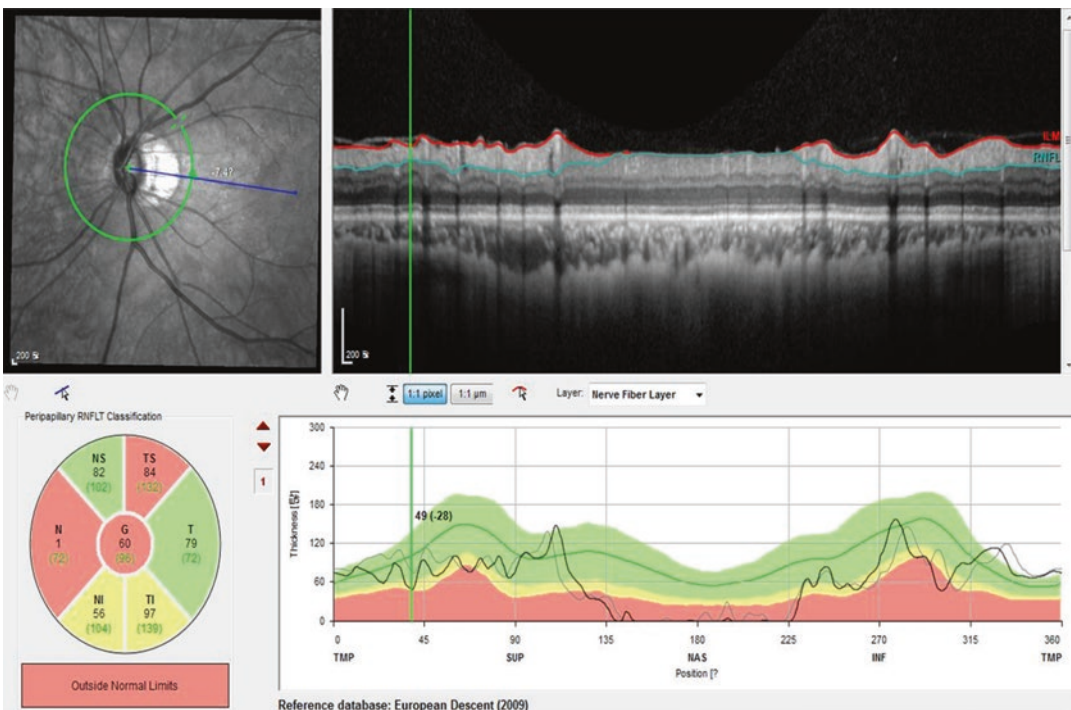


Fig. 16 Segmentation artifact in Spectralis OCT imaging of RNFL in a patient with myopic tilted disc. An incorrectly segmented posterior RNFL led to an RNFL thickness measurement of zero at the nasal quadrant

5.3 Incorrect Scan-Circle Placement

Incorrect RNFL scan-circle placement is easily identifiable on the final printout. Although most

of these artifacts have been reported to be mild, moderate-to-severe displacement of the circle may result in erroneous RNFL values (Asrani et al. 2014; Cheung et al. 2008) (Fig. 17).

a

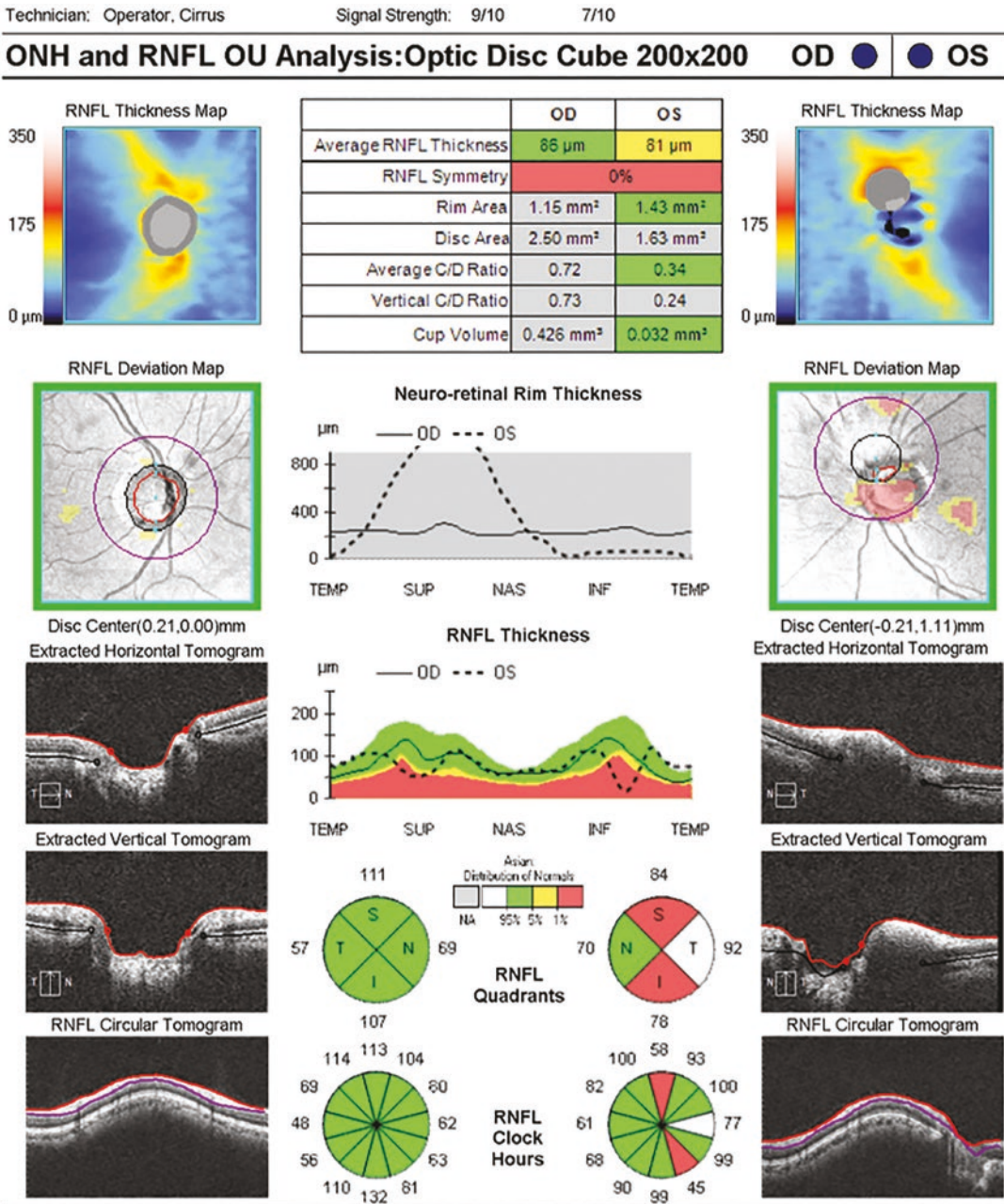


Fig. 17 (a) Incorrect RNFL circle resulting in artifacts of the RNFL thickness notwithstanding acceptable signal strength. (b) After replacing the RNFL circle, the RNFL thickness was within normal range

b

Technician: Operator, Cirrus

Signal Strength: 8/10

6/10

ONH and RNFL OU Analysis: Optic Disc Cube 200x200 OD ● ● OS

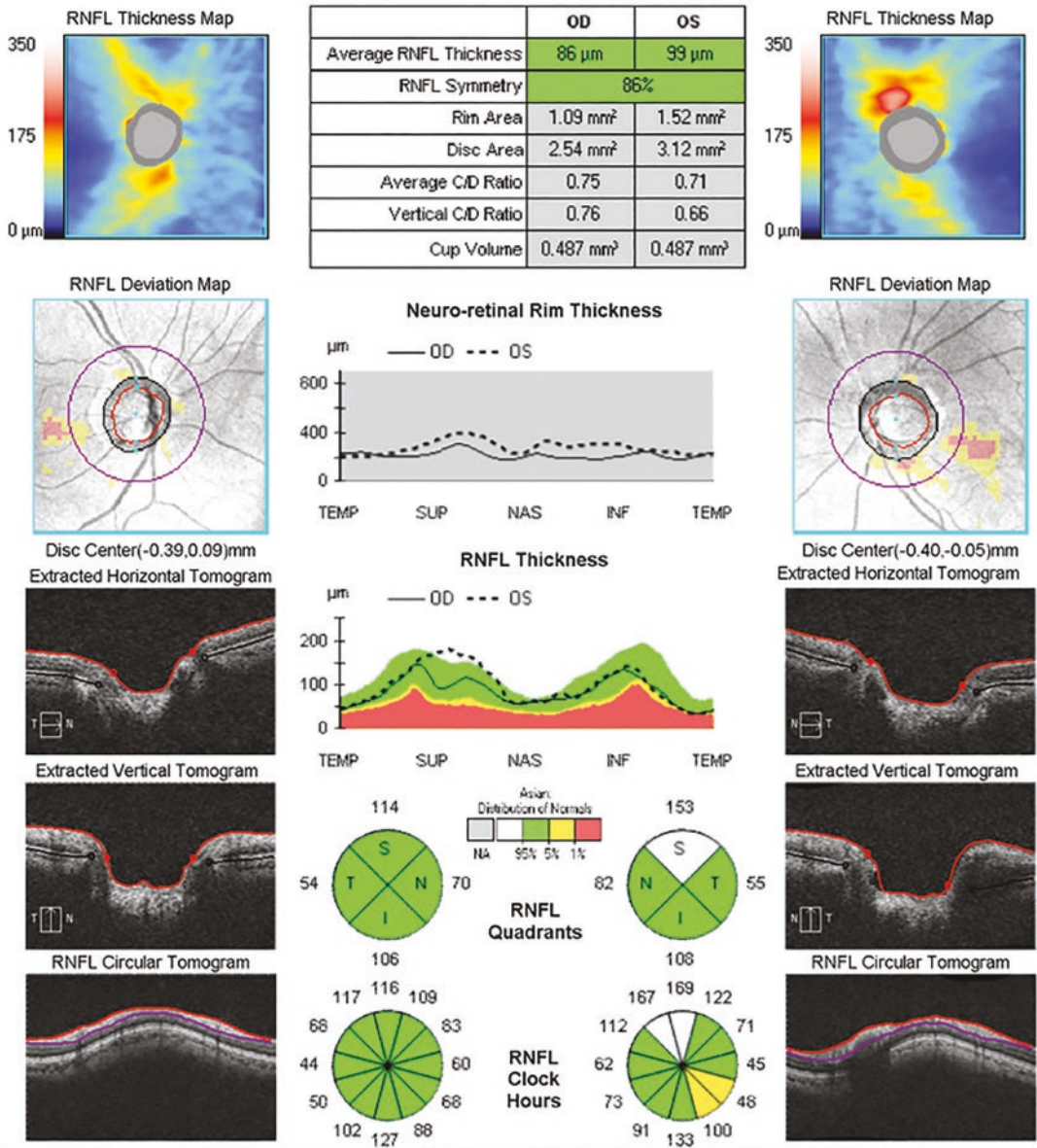


Fig. 17 (continued)

5.4 Incorrect Axial Alignment of OCT Image

Improper axial alignment of the scan in the z-axis occurs when the ocular structures are only

partially included within the acquisition frame, resulting in image truncation (i.e., all edges of the image were not within the acquisition window). The areas of absolute loss on the RNFL thickness plot result in erroneous mean measure-

Technician: Operator, Cirrus

Signal Strength: 6/10

6/10

ONH and RNFL OU Analysis: Optic Disc Cube 200x200 OD ● ● OS

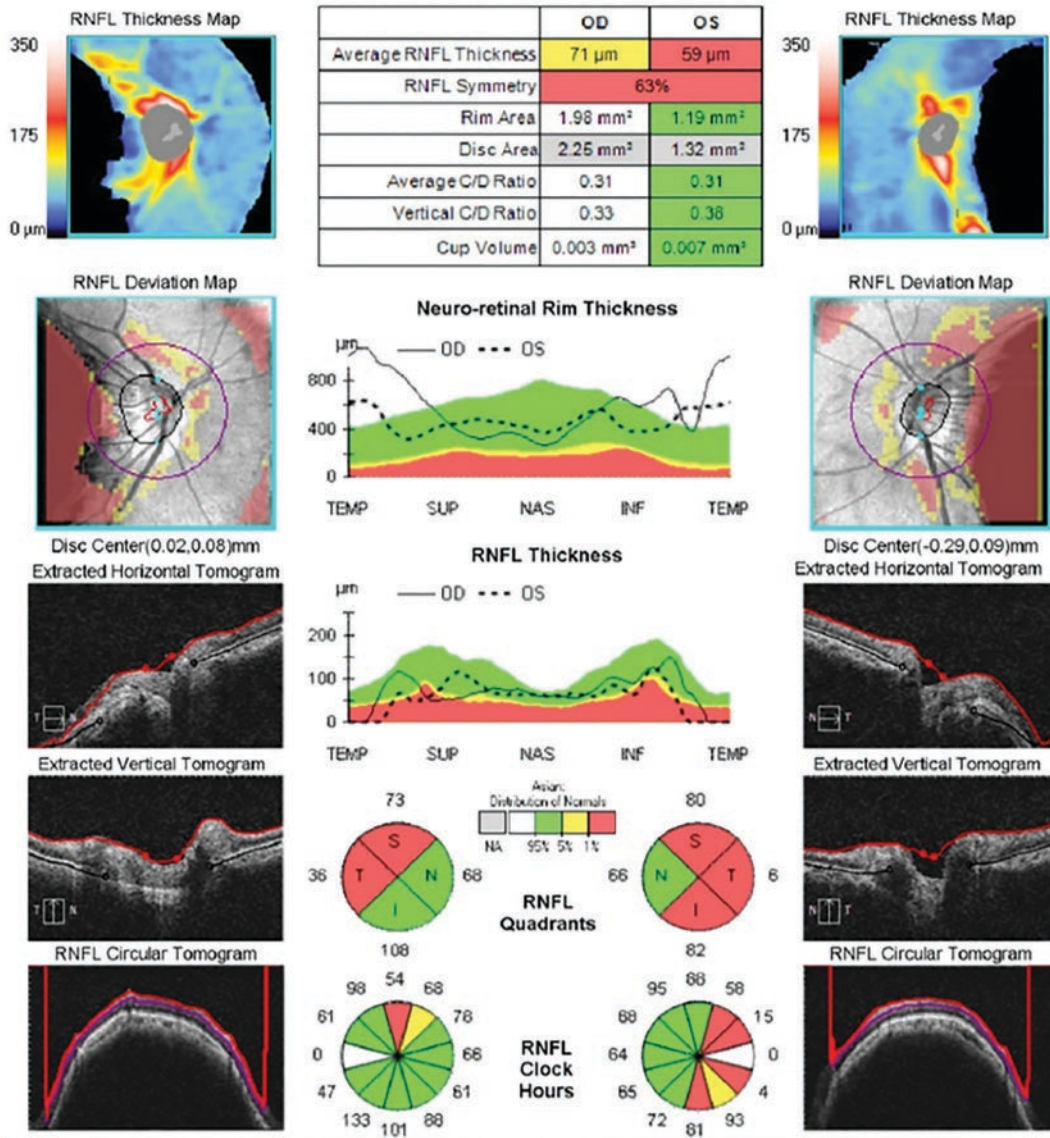


Fig. 18 Truncation of RNFL data due to decentering on z-axis. This resulted in regional errors in the derived RNFL thickness, which can be seen as irregular black

areas of absolute thinning on the RNFL thickness map. Both eyes are predisposed to this z-axis truncation because of the presence of steep retinal curvature in myopic eyes

ments in the sector and in the global mean RNFL thickness values (Fig. 18). A clue to identifying such artifacts is the presence of RNFL values less than 30 μm or near zero. OCT image truncation commonly occurs in myopic eyes with a steep retinal curvature or in glaucomatous eyes with deep cupping, because the peripapillary

RNFL may be difficult to capture on a single B-scan, due to the differences in height between the opposite sides of the circular RNFL scan. Other causes include improper distance between the eye and the device due to incorrect patient positioning and axial misalignment of the OCT scanning head.

6 OCT Artifacts in GCIPL Analysis

6.1 Macular GCIPL

Various studies have reported the prevalence of errors of RNFL and macular scans. Li and associates (2020) reported that artifacts were more common on peripapillary RNFL scans (43.7%) than on macular scans (30.0%), and Liu et al. (2015) reported a similar prevalence of RNFL artifacts (i.e., on 46.3% of scans). Asrani and associates (2014) reported that artifacts were more common on the macular scan (28.2%) than on the peripapillary RNFL scan (19.97%).

The commercially available segmentation algorithms are prone to segmentation failures of the GCIPL complex. Errors in segmentation occur in low-signal-strength scans, optic nerve edema, or in the cases of outer-retinal-layer structural abnormalities that affect segmentation of the inner retinal layers (Lee et al. 2010; Garvin et al. 2008). One sign of inaccurate inner-layer segmentation is the appearance of a non-pathologic shape, such as a corner of abnormal thinning, on the thickness and probability maps. Errors often appear as segments of blue (thinning) on the thickness map (Fig. 19). A GCIPL reading of less than 40 μm is also typically indicative of areas of segmentation error. On the B-scan, the algorithm's identification of the boundaries of the ganglion cell layer and inner plexiform layer often collapse together in the

areas of artifact, thereby producing artifactual thinning.

Macular scan artifacts more commonly have been associated with dry eye or corneal opacities. The effect of corneal drying degrades many images including stereo disc photos (Stein et al. 2006). Encouraging the patient to blink may help improve the signal strength and reduce artifacts.

6.2 Interindividual Variation of Retinal Ganglion Cell Thickness Within Macula

In the macula thickness profile of normal eyes, the perifoveal location is the most variable site due to a wide variation in the thickness profile of the inner retina immediately surrounding the fovea. Therefore, an abnormal probability map in the perifoveal location should be spotlighted carefully and correlated with the clinical exam and functional tests. It is important to ensure that the fovea is correctly identified and centered by the OCT analysis. Otherwise, this may lead to artifactual thickening and thinning displayed as abnormal. However, true atrophy of the GCIPL may also cause perifoveal thinning and enlargement of the foveal depression, which renders difficult the differentiation of focal pathological thinning from normal variation in the perifoveal location (Chen and Kardon 2016).

Technician: Signal Strength: 6/10 7/10

Ganglion Cell OU Analysis: Macular Cube 200 · 200

OD OS

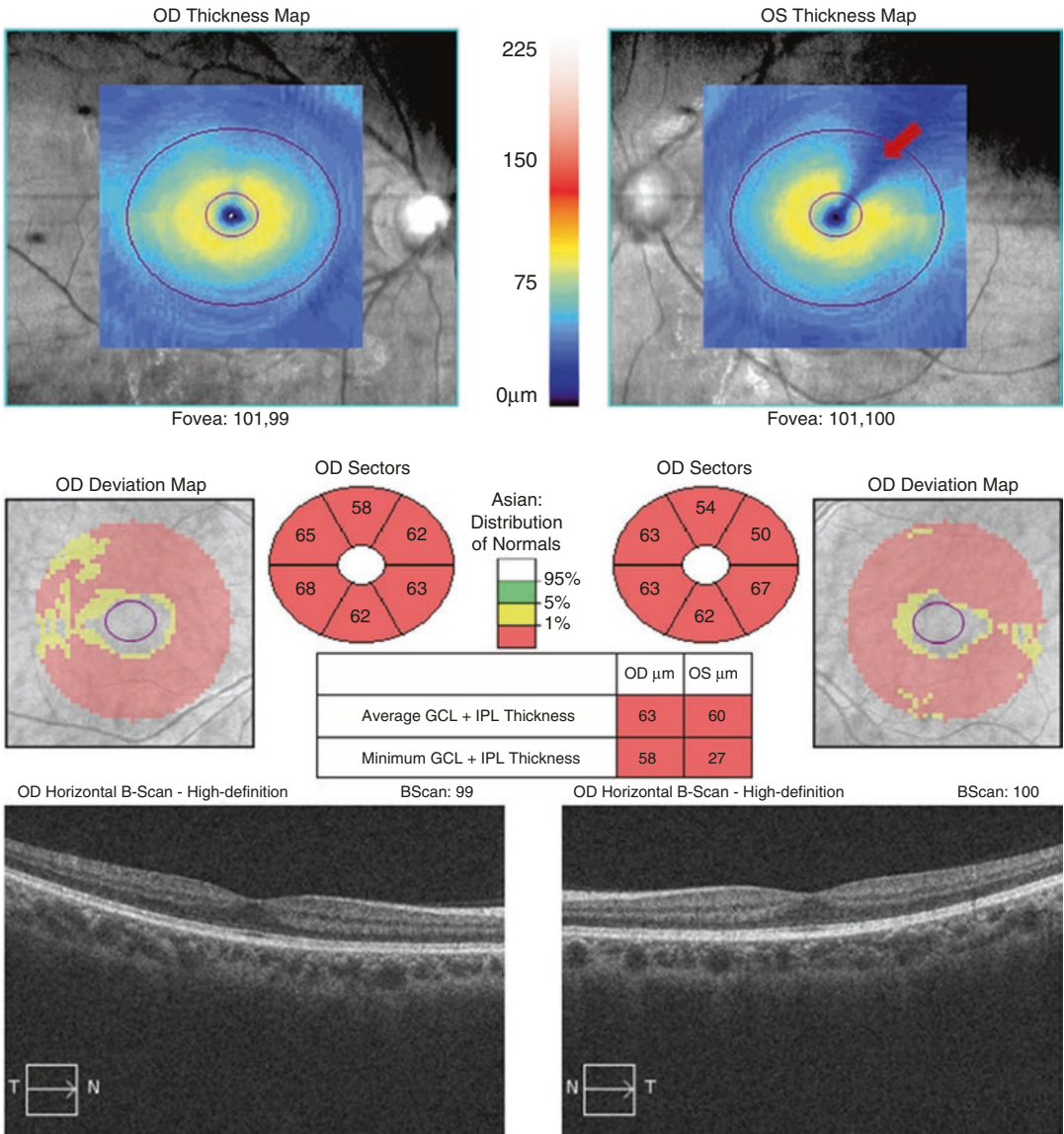


Fig. 19 Artificially decreased GCIPL complex thickness due to errors in segmentation. This can be seen as a segment of blue “thinning” on the thickness map (red arrow).

The minimum thickness of GCIPL thickness is less than 40 μm in the left eye, which also is often an indication of segmentation error

References

- Anwar Z, Wellik SR, Galor A. Glaucoma therapy and ocular surface disease: current literature and recommendations. *Curr Opin Ophthalmol*. 2013;24(2):136–43. <https://doi.org/10.1097/ICU.0b013e32835c8aba>.
- Asrani S, Essaid L, Alder BD, Santiago-Turla C. Artifacts in spectral-domain optical coherence tomography measurements in glaucoma. *JAMA Ophthalmol*. 2014;132(4):396–402. <https://doi.org/10.1001/jamaophthalmol.2013.7974>.
- Bambo MP, Garcia-Martin E, Otin S, et al. Influence of cataract surgery on repeatability and measurements of spectral domain optical coherence tomography. *Br J Ophthalmol*. 2014;98(1):52. <https://doi.org/10.1136/bjophthalmol-2013-303752>.
- Bayer A, Akman A. Artifacts and anatomic variations in optical coherence tomography. *Turk J Ophthalmol*. 2020;50(2):99–106. <https://doi.org/10.4274/tjo.galenos.2019.78000>.
- Bayraktar S, Cebeci Z, Kabaalioglu M, Ciloglu S, Kir N, Izgi B. Peripapillary retinoschisis in glaucoma patients. *J Ophthalmol*. 2016;2016:1612720. <https://doi.org/10.1155/2016/1612720>.
- Bennett AG, Rudnicka AR, Edgar DF. Improvements on Littmann's method of determining the size of retinal features by fundus photography. *Graefes Arch Clin Exp Ophthalmol*. 1994;32(6):361–7. <https://doi.org/10.1007/BF00175988>.
- Budenz DL, Anderson DR, Varma R, et al. Determinants of normal retinal nerve fiber layer thickness measured by Stratus OCT. *Ophthalmology*. 2007;114(6):1046–52. <https://doi.org/10.1016/j.ophtha.2006.08.046>.
- Celebi AR, Mirza GE. Age-related change in retinal nerve fiber layer thickness measured with spectral domain optical coherence tomography. *Invest Ophthalmol Vis Sci*. 2013;54(13):8095–103. <https://doi.org/10.1167/iops.13-12634>.
- Chan CK, Miller NR. Peripapillary nerve fiber layer thickness measured by optical coherence tomography in patients with no light perception from long-standing nonglaucomatous optic neuropathies. *J Neuro-ophthalmol*. 2007;27(3):176–9. <https://doi.org/10.1097/WNO.0b013e31814b1ac4>.
- Chen JJ, Kardon RH. Avoiding Clinical misinterpretation and artifacts of optical coherence tomography analysis of the optic nerve, retinal nerve fiber layer, and ganglion cell layer. *J Neuro-ophthalmol*. 2016;36(4):417–38. <https://doi.org/10.1097/wno.0000000000000422>.
- Cheung CY, Leung CK, Lin D, Pang CP, Lam DS. Relationship between retinal nerve fiber layer measurement and signal strength in optical coherence tomography. *Ophthalmology*. 2008;115(8):1347–51. <https://doi.org/10.1016/j.ophtha.2007.11.027>.
- Chong GT, Lee RK. Glaucoma versus red disease: imaging and glaucoma diagnosis. *Curr Opin Ophthalmol*. 2012;23(2):79–88. <https://doi.org/10.1097/ICU.0b013e32834ff431>.
- Colen TP, Lemij HG. Prevalence of split nerve fiber layer bundles in healthy eyes imaged with scanning laser polarimetry. *Ophthalmology*. 2001;108(1):151–6. [https://doi.org/10.1016/S0161-6420\(00\)00516-9](https://doi.org/10.1016/S0161-6420(00)00516-9).
- Congdon N, Vingerling JR, Klein BE, et al. Prevalence of cataract and pseudophakia/aphakia among adults in the United States. *Arch Ophthalmol (Chicago, Ill: 1960)*. 2004;122(4):487–94. <https://doi.org/10.1001/archophth.122.4.487>.
- Curcio CA, Saunders PL, Younger PW, Malek G. Peripapillary chorioretinal atrophy: Bruch's membrane changes and photoreceptor loss. *Ophthalmology*. 2000;107(2):334–43. [https://doi.org/10.1016/s0161-6420\(99\)00037-8](https://doi.org/10.1016/s0161-6420(99)00037-8).
- Dong ZM, Wollstein G, Schuman JS. Clinical utility of optical coherence tomography in glaucoma. *Invest Ophthalmol Vis Sci*. 2016;57(9):Oct556–67. <https://doi.org/10.1167/iops.16-19933>.
- Gabriele ML, Wollstein G, Ishikawa H, et al. Optical coherence tomography: history, current status, and laboratory work. *J Invest Ophthalmol Visual Sci*. 2011;52(5):2425–36. <https://doi.org/10.1167/iops.10-6312>.
- Garvin MK, Abramoff MD, Kardon R, Russell SR, Wu X, Sonka M. Intraretinal layer segmentation of macular optical coherence tomography images using optimal 3-D graph search. *IEEE Trans Med Imaging*. 2008;27(10):1495–505. <https://doi.org/10.1109/tmi.2008.923966>.
- Giani A, Cigada M, Choudhry N, et al. Reproducibility of retinal thickness measurements on normal and pathologic eyes by different optical coherence tomography instruments. *Am J Ophthalmol*. 2010;150(6):815–24. <https://doi.org/10.1016/j.ajo.2010.06.025>.
- Groth SL, Harrison A, Grajewski AL, Lee MS. Retinal nerve fiber layer thickness using spectral-domain optical coherence tomography in patients with no light perception secondary to optic atrophy. *J Neuro-ophthalmol*. 2013;33(1):37–9. <https://doi.org/10.1097/WNO.0b013e318272c7cd>.
- Han IC, Jaffe GJ. Evaluation of artifacts associated with macular spectral-domain optical coherence tomography. *Ophthalmology*. 2010;117(6):1177–89.e4. <https://doi.org/10.1016/j.ophtha.2009.10.029>.
- Hollander DA, Barricks ME, Duncan JL, Irvine AR. Macular schisis detachment associated with angle-closure glaucoma. *Arch Ophthalmol (Chicago, Ill: 1960)*. 2005;123(2):270–2. <https://doi.org/10.1001/archophth.123.2.270>.
- Hong SW, Ahn MD, Kang SH, Im SK. Analysis of peripapillary retinal nerve fiber distribution in normal young adults. *J Invest Ophthalmol Vis Sci*. 2010;51(7):3515–23. <https://doi.org/10.1167/iops.09-4888>.
- Hood DC, Salant JA, Arthur SN, Ritch R, Liebmann JM. The location of the inferior and superior tem-

- poral blood vessels and interindividual variability of the retinal nerve fiber layer thickness. *J Glaucoma*. 2010;19(3):158–66. <https://doi.org/10.1097/IJG.0b013e3181af31ec>.
- Huang J, Liu X, Wu Z, Sadda S. Image quality affects macular and retinal nerve fiber layer thickness measurements on fourier-domain optical coherence tomography. *Ophthalm Surg Lasers Imag*. 2011;42(3):216–21. <https://doi.org/10.3928/15428877-20110324-01>.
- Hwang YH, Lee JY, Kim YY. The effect of head tilt on the measurements of retinal nerve fibre layer and macular thickness by spectral-domain optical coherence tomography. *Br J Ophthalmol*. 2011;95(11):1547–51. <https://doi.org/10.1136/bjo.2010.194118>.
- Hwang YH, Yoo C, Kim YY. Characteristics of peripapillary retinal nerve fiber layer thickness in eyes with myopic optic disc tilt and rotation. *J Glaucoma*. 2012;21(6):394–400. <https://doi.org/10.1097/IJG.0b013e3182182567>.
- Hwang YH, Kim YY, Kim HK, Sohn YH. Effect of peripapillary retinoschisis on retinal nerve fibre layer thickness measurement in glaucomatous eyes. *Br J Ophthalmol*. 2014;98(5):669–74. <https://doi.org/10.1136/bjophthalmol-2013-303931>.
- Inoue M, Bissen-Miyajima H, Yoshino M, Suzuki T. Wavy horizontal artifacts on optical coherence tomography line-scanning images caused by diffractive multifocal intraocular lenses. *J Cataract Refract Surg*. 2009;35(7):1239–43. <https://doi.org/10.1016/j.jcrs.2009.04.016>.
- Jonas JB, Nguyen XN, Gusek GC, Naumann GO. Parapapillary chorioretinal atrophy in normal and glaucoma eyes. I. Morphometric data. *Invest Ophthalmol Vis Sci*. 1989;30(5):908–18.
- Kahook MY, Noecker RJ, Ishikawa H, et al. Peripapillary schisis in glaucoma patients with narrow angles and increased intraocular pressure. *Am J Ophthalmol*. 2007;143(4):697–9. <https://doi.org/10.1016/j.ajo.2006.10.054>.
- Kaliner E, Cohen MJ, Miron H, Kogan M, Blumenthal EZ. Retinal nerve fiber layer split bundles are true anatomic variants. *Ophthalmology*. 2007;114(12):2259–64. <https://doi.org/10.1016/j.ophtha.2007.01.028>.
- Kang SH, Hong SW, Im SK, Lee SH, Ahn MD. Effect of myopia on the thickness of the retinal nerve fiber layer measured by cirrus HD optical coherence tomography. *J Invest Ophthalmol Vis Sci*. 2010;51(8):4075–83. <https://doi.org/10.1167/iovs.09-4737>.
- Kim SY, Park H-YL, Park CK. The effects of peripapillary atrophy on the diagnostic ability of stratus and cirrus OCT in the analysis of optic nerve head parameters and disc size. *J Invest Ophthalmol Vis Sci*. 2012;53(8):4475–84. <https://doi.org/10.1167/iovs.12-9682>.
- Lee K, Niemeijer M, Garvin MK, Kwon YH, Sonka M, Abramoff MD. Segmentation of the optic disc in 3-D OCT scans of the optic nerve head. *IEEE Trans Med Imaging*. 2010;29(1):159–68. <https://doi.org/10.1109/TMI.2009.2031324>.
- Leung CK, Mohamed S, Leung KS, et al. Retinal nerve fiber layer measurements in myopia: an optical coherence tomography study. *Invest Ophthalmol Vis Sci*. 2006;47(12):5171–6. <https://doi.org/10.1167/iovs.06-0545>.
- Leung CK, Cheng AC, Chong KK, et al. Optic disc measurements in myopia with optical coherence tomography and confocal scanning laser ophthalmoscopy. *Invest Ophthalmol Vis Sci*. 2007;48(7):3178–83. <https://doi.org/10.1167/iovs.06-1315>.
- Leung CKS, Ye C, Weinreb RN, Yu M, Lai G, Lam DS. Impact of age-related change of retinal nerve fiber layer and macular thicknesses on evaluation of glaucoma progression. *Ophthalmology*. 2013;120(12):2485–92. <https://doi.org/10.1016/j.ophtha.2013.07.021>.
- Li A, Thompson AC, Asrani S. Impact of Artifacts from optical coherence tomography retinal nerve fiber layer and macula scans on detection of glaucoma progression. *Am J Ophthalmol*. 2020;221:235–45. <https://doi.org/10.1016/j.ajo.2020.08.018>.
- Liu Y, Simavli H, Que CJ, et al. Patient characteristics associated with artifacts in Spectralis optical coherence tomography imaging of the retinal nerve fiber layer in glaucoma. *Am J Ophthalmol*. 2015;159(3):565–76.e2. <https://doi.org/10.1016/j.ajo.2014.12.006>.
- Manjunath V, Shah H, Fujimoto JG, Duker JS. Analysis of peripapillary atrophy using spectral domain optical coherence tomography. *Ophthalmology*. 2011;118(3):531–6. <https://doi.org/10.1016/j.ophtha.2010.07.013>.
- Massa GC, Vidotti VG, Cremasco F, Lupinacci APC, Costa VP. Influence of pupil dilation on retinal nerve fibre layer measurements with spectral domain OCT. *Eye*. 2010;24(9):1498–502. <https://doi.org/10.1038/eye.2010.72>.
- Moore DB, Jaffe GJ, Asrani S. Retinal nerve fiber layer thickness measurements: uveitis, a major confounding factor. *Ophthalmology*. 2015;122(3):511–7. <https://doi.org/10.1016/j.ophtha.2014.09.008>.
- Mwanza JC, Borhade AM, Sekhon N, et al. Effect of cataract and its removal on signal strength and peripapillary retinal nerve fiber layer optical coherence tomography measurements. *J Glaucoma*. 2011;20(1):37–43. <https://doi.org/10.1097/IJG.0b013e3181ccb93b>.
- Mwanza JC, Budenz DL, Warren JL, et al. Retinal nerve fibre layer thickness floor and corresponding functional loss in glaucoma. *Br J Ophthalmol*. 2015;99(6):732–7. <https://doi.org/10.1136/bjophthalmol-2014-305745>.
- Örnek N, Büyüktortop N, Örnek K. Peripapillary and macular retinoschisis in a patient with pseudoexfoliation glaucoma. *BMJ Case Reports*.

- 2013;2013:bcr2013009469. <https://doi.org/10.1136/bcr-2013-009469>.
- Parikh RS, Parikh SR, Sekhar GC, Prabakaran S, Babu JG, Thomas R. Normal age-related decay of retinal nerve fiber layer thickness. *Ophthalmology*. 2007;114(5):921–6. <https://doi.org/10.1016/j.ophtha.2007.01.023>.
- Qiu KL, Zhang MZ, Leung CK, et al. Diagnostic classification of retinal nerve fiber layer measurement in myopic eyes: a comparison between time-domain and spectral-domain optical coherence tomography. *Am J Ophthalmol*. 2011;152(4):646–53.e2. <https://doi.org/10.1016/j.ajo.2011.04.002>.
- Rao HL, Addepalli UK, Yadav RK, Senthil S, Choudhari NS, Garudadri CS. Effect of Scan Quality on Diagnostic Accuracy of Spectral-Domain Optical Coherence Tomography in Glaucoma. *Am J Ophthalmol*. 2014;157(3):719–27.e1. <https://doi.org/10.1016/j.ajo.2013.12.012>.
- Roh S, Noecker RJ, Schuman JS, Hedges TR 3rd, Weiter JJ, Mattox C. Effect of optic nerve head drusen on nerve fiber layer thickness. *Ophthalmology*. 1998;105(5):878–85. [https://doi.org/10.1016/S0161-6420\(98\)95031-X](https://doi.org/10.1016/S0161-6420(98)95031-X).
- Russell DJ, Fallah S, Loer CJ, Riffenburgh RH. A comprehensive model for correcting RNFL readings of varying signal strengths in cirrus optical coherence tomography. *J Invest Ophthalmol Vis Sci*. 2014;55(11):7297–302. <https://doi.org/10.1167/iovs.14-14993>.
- Savini G, Zanini M, Barboni P. Influence of pupil size and cataract on retinal nerve fiber layer thickness measurements by Stratus OCT. *J Glaucoma*. 2006;15(4):336–40. <https://doi.org/10.1097/01.jgg.0000212244.64584.c2>.
- Savini G, Carbonelli M, Parisi V, Barboni P. Effect of pupil dilation on retinal nerve fibre layer thickness measurements and their repeatability with Cirrus HD-OCT. *Eye (London, England)*. 2010;24(9):1503–8. <https://doi.org/10.1038/eye.2010.66>.
- Savini G, Barboni P, Parisi V, Carbonelli M. The influence of axial length on retinal nerve fibre layer thickness and optic-disc size measurements by spectral-domain OCT. *Br J Ophthalmol*. 2012;96(1):57–61. <https://doi.org/10.1136/bjo.2010.196782>.
- Savino PJ, Glaser JS, Rosenberg MA. A clinical analysis of pseudopapilledema. II. Visual field defects. *Arch Ophthalmol (Chicago, Ill: 1960)*. 1979;97(1):71–5. <https://doi.org/10.1001/archoph.1979.010200100011002>.
- Sayed MS, Margolis M, Lee RK. Green disease in optical coherence tomography diagnosis of glaucoma. *Curr Opin Ophthalmol*. 2017;28(2):139–53.
- Stein DM, Wollstein G, Ishikawa H, Hertzmark E, Noecker RJ, Schuman JS. Effect of corneal drying on optical coherence tomography. *Ophthalmology*. 2006;113(6):985–91. <https://doi.org/10.1016/j.ophtha.2006.02.018>.
- Stein JD, Talwar N, Laverne AM, Nan B, Lichter PR. Trends in use of ancillary glaucoma tests for patients with open-angle glaucoma from 2001 to 2009. *Ophthalmology*. 2012;119(4):748–58. <https://doi.org/10.1016/j.ophtha.2011.09.045>.
- Strouthidis NG, Yang H, Downs JC, Burgoyne CF. Comparison of clinical and three-dimensional histomorphometric optic disc margin anatomy. *J Invest Ophthalmol Vis Sci*. 2009a;50(5):2165–74. <https://doi.org/10.1167/iovs.08-2786>.
- Strouthidis NG, Yang H, Fortune B, Downs JC, Burgoyne CF. Detection of optic nerve head neural canal opening within histomorphometric and spectral domain optical coherence tomography data sets. *J Invest Ophthalmol Vis Sci*. 2009b;50(1):214–23. <https://doi.org/10.1167/iovs.08-2302>.
- Sull AC, Vuong LN, Price LL, et al. Comparison of spectral/Fourier domain optical coherence tomography instruments for assessment of normal macular thickness. *Retina (Philadelphia, Pa)*. 2010;30(2):235–45. <https://doi.org/10.1097/IAE.0b013e3181bd2c3b>.
- Taibbi G, Peterson GC, Syed MF, Vizzeri G. Effect of motion artifacts and scan circle displacements on cirrus HD-OCT retinal nerve fiber layer thickness measurements. *J Invest Ophthalmol Vis Sci*. 2014;55(4):2251–8. <https://doi.org/10.1167/iovs.13-13276>.
- Vizzeri G, Bowd C, Medeiros FA, Weinreb RN, Zangwill LM. Effect of signal strength and improper alignment on the variability of stratus optical coherence tomography retinal nerve fiber layer thickness measurements. *Am J Ophthalmol*. 2009;148(2):249–55.e1. <https://doi.org/10.1016/j.ajo.2009.03.002>.
- Wang G, Qiu KL, Lu XH, et al. The effect of myopia on retinal nerve fibre layer measurement: a comparative study of spectral-domain optical coherence tomography and scanning laser polarimetry. *Br J Ophthalmol*. 2011;95(2):255–60. <https://doi.org/10.1136/bjo.2009.176768>.
- Weinreb RN, Aung T, Medeiros FA. The pathophysiology and treatment of glaucoma: a review. *JAMA*. 2014;311(18):1901–11. <https://doi.org/10.1001/jama.2014.3192>.
- Wu Z, Vazeen M, Varma R, et al. Factors associated with variability in retinal nerve fiber layer thickness measurements obtained by optical coherence tomography. *Ophthalmology*. 2007;114(8):1505–12. <https://doi.org/10.1016/j.ophtha.2006.10.061>.
- Yamashita T, Asaoka R, Tanaka M, et al. Relationship between position of peak retinal nerve fiber layer thickness and retinal arteries on sectoral retinal nerve fiber layer thickness. *J Invest Ophthalmol Vis Sci*. 2013;54(8):5481–8. <https://doi.org/10.1167/iovs.12-11008>.

- Yamashita T, Kii Y, Tanaka M, et al. Relationship between supernormal sectors of retinal nerve fibre layer and axial length in normal eyes. *Acta Ophthalmol.* 2014;92(6):e481–7. <https://doi.org/10.1111/aos.12382>.
- Yoo YC, Lee CM, Park JH. Changes in peripapillary retinal nerve fiber layer distribution by axial length. *Optom Vis Sci.* 2012;89(1):4–11. <https://doi.org/10.1097/OPX.0b013e3182358008>.
- Zhao M, Li X. Macular retinoschisis associated with normal tension glaucoma. *Graefe's Arch Clin Exp Ophthalmol.* 2011;249(8):1255–8. <https://doi.org/10.1007/s00417-011-1668-y>.